Granular Matter 1, 163–181 © Springer-Verlag 1999

A constitutive model of multiphase mixtures and its application in shearing flows of saturated solid-fluid mixtures

Yongqi Wang, Kolumban Hutter

Abstract A continuum theory of a multiphase mixture is formulated. In the basic balance laws we introduce an additional balance of equilibrated forces to describe the microstructural response according to Goodman & Cowin [11] and Passman et al. [23] for each constituent. Based on the Müller-Liu form of the second law of thermodynamics a set of constitutive equations for a viscous solid-fluid mixture with microstructure is derived. These relatively general equations are then reduced to a system of ordinary differential equations describing a steady flow of the solid-fluid mixture between two horizontal plates. The resulting boundary value problem is solved numerically and results are presented for various values of parameters and boundary conditions. It is shown that simple shearing generally does not occur. Typically, for the solid phase, in the vicinity of a boundary, if the solid-volume fraction is low, a layer of high shear rate occurs, whose thickness is nearly between 5 and 15 grain diameters, while if the solid-volume fraction is high, an interlock phenomenon occurs. The fluid velocity depends largely on the drag force between the constituents. If the drag coefficient is sufficiently large, the fluid flow is nearly the same as that of the solid, while for a small drag coefficient, the fluid shearing flow largely decouples from that of the solid in the entire flow region. Apart from this, there is a tendency for solid particles to accumulate in regions of low shear rate.

Key words Solid-fluid mixture, Constitutive equations, Shearing flow

Received: 30 June 1998

Y. Wang, K. Hutter
Institute of Mechanics, Darmstadt University of Technology
Hochschulstr. 1, D-64289 Darmstadt, Germany
e-mail: wang@mechanik.tu-darmstadt.de,
e-mail: hutter@mechanik.tu-darmstadt.de

Correspondence to: K. Hutter

The authors want to thank for financial support by the Deutsche Forschungagemeinschaft within the Special Collaborative Program (SFB) 298. Prof. Dr. K. Wilmanski's review of the manscript is appreciated.

1 Introduction

The mechanics of multiphase mixtures is of fundamental importance in several fields of engineering, i.e., debris flows, soil mechanics, ground water engineering, sediment transport as well as many other fields in mechanical and chemical engineering. In this work our major interest is in granular-fluid mixtures. Such a material is a collection of a large number of discrete solid particles with interstices filled with a fluid or a gas. In most flows involving granular materials, the interstitial fluid plays an insignificant role in the transportation of momentum, and thus flows of such materials can be considered dispersed single phase rather than multiphase flows. A detailed review of flows of single granular materials has been presented by Hutter & Rajagopal [14].

It is widely known today that granular media exhibit microstructural effects on their macroscale, which is accounted for, in general, by adding an additional dynamical equation for the solid volume fraction ν_s. Different authors do not unanimously agree upon the form of this equation. Svendsen & Hutter [26] treated the solid-volume fraction as an internal variable and write an evolution equation balancing its time rate of change with its production. Wilmanski [32] on the other hand, using statistical arguments on the microscale demonstrated that the Svendsen-Hutter equation needed to be complemented by a flux term, thus arriving at a complete balance law. On the other hand, almost 25 years ago, Goodman & Cowin [11] were, based on the theory of structured media, introducing a balance law of equilibrated forces in which second time derivatives of ν_s, i.e., $\ddot{\nu}_s$ were balanced with a flux, a production and supply term.

In some occasions or when the mass of the interstitial fluid is comparable to that of the solids the interactions between the fluid and solid phases are significant, one should study these flow problems by employing the theory of multiphase flows. Study of multiphase flow has attracted considerable attention in the past thirty years. Some detailed reviews of solid-fluid mixtures have been presented by Hutter et al. [15] and Takahashi [28]. The large number of articles published on fluid-solid flows typically employ one of two theories, (i) averaging or (ii) mixture theory. In the averaging approach, equations of motion, valid for a single constituent, are modified to account for the presence of the other components and

the interactions between components. These equations are then averaged over time or volume, which are large compared with a characteristic particle dimension or a typical microscale period but small compared to dimensions of the whole system. From the viewpoint of mathematical manipulation of the averaged quantities, a number of terms arise, which are usually interpreted as some form of interaction between the constituents. Constitutive relations to represent these terms and the stress tensors for each constituent are required. The second method of modeling multicomponent systems is mixture theory. The fundamental assumption of the theory is that, at any instant of time, every point in space is occupied by one particle from each constituent. Ahmadi [1, 2], Bluhm et al. [5], Bowen [6, 7], Ehlers [9, 10], Homsy et al. [13], Johnson et al. [16], Massoudi [19], Passman et al. [23, 24], Svendsen & Hutter [26] and Svendsen [27] have used such an approach for modeling mixture systems. Like averaging, mixture theory also requires constitutive relations for the stress tensors of each component of the mixture and for momentum exchange between the components.

In deriving their reduced constitutive relations from a class of constitutive postulates for a solid-fluid mixture Passman et al., following the approach of Goodman & Cowin [11] for dry granular materials, employed the principle of equilibrated stresses and introduced additional balances for each constituent to describe the microstructural response. They used the Coleman-Noll approach of thermodynamics, i.e., the linear momentum equation, the energy balance and the balance of equilibrated forces for each constituent had all arbitrarily assignable external source terms, so that these balance laws would not affect the exploitation of the entropy inequality. Whereas such a procedure can be tolerated for the momentum and energy sources, it is physically not justified for the balance law of equilibrated forces. This is an internal law all by itself, and at least this law must influence the thermodynamics.

This is one reason why we have rederived the thermodynamic mixture theory, now using the Müller-Liu approach in which the entropy inequality is exploited *for all thermodynamic processes*, i.e., by using all balance laws as constraints, be these processes driven by external sources or not. We find that our derived results do not agree with those of Passman et al. In our more general approach there are additional terms in the constitutive relations e.g. of stress not contained in Passman et al.'s model. These additional terms turn out to be physically significant.

The present theory is believed to be valid for the full spectrum of two phase solid-fluid media covering the range of variation of the solid-volume fraction from the high values in the granular media to the low values in the low concentration suspension flows. The theory allows also the possibility of supporting shear stress at the equilibrium state which is necessary for granular media and has e.g. been observed in the case of high concentration suspensions such as blood.

In section 2, the basic laws of motion for each constituent and the entropy inequality for the mixture are presented. Section 3 is devoted to the derivation of the constitutive equations of multiphase media from thermodynamic considerations of the first and second law. In section 4 the basic equations of motion of the fluid and solid phases are presented when these constituents (for themselves) are volume preserving. In order to assess the implications of the theory, we consider in section 5 a specific boundary-value problem. By use of a special expression of free energy for each constituent used in Passman et al. [24], the theory is applied to analyses of steady fully-developed horizontal shearing flow of solid-fluid media between two parallel plates, one of which is held stationary, the other of which is moved at a constant speed. The boundary value problem is solved using the method of successive approximation. We find that our partial numerical results are qualitatively very similar to those obtained by Passman et al. [24], although the constitutive equations of both models are not the same. Results show that the solid particles tend to concentrate themselves near the centerline of the flow and the velocity profile is nonlinear, with the shearing highest in the regions of low particle concentration, i.e., near the bounding plates. These results are dependent on boundary conditions; however, they are in qualitative agreement with experimental results on high concentration suspensions [3, 4, 12]. In section 6, this paper is summarized.

2 Thermodynamic processes

2.1 Balance relations

We begin by assuming that the mixture consists of N constituents. The index $\mathfrak{a}$ denotes the $\mathfrak{a}$-th constituent, $\mathfrak{a} = 1, \ldots, N$. The necessary thermal and mechanical field variables for each constituent are introduced as primitive quantities. Specifically, there exists a kinematic variable, the *volume fraction* or *volume distribution function* $\nu_\mathfrak{a}$ for each constituent $\mathfrak{a}$, introduced originally by Goodman & Cowin [11] for dry granular materials, that accounts for the distributions of volume of each constituent $\mathfrak{a}$ in a multiphase mixture. It is complemented by the distributed mass density (granular true mass density) $\gamma_\mathfrak{a}$, the stress tensor $\boldsymbol{T}_\mathfrak{a}$, body force $\boldsymbol{b}_\mathfrak{a}$, specific internal energy $\varepsilon_\mathfrak{a}$, heat flux vector $\boldsymbol{q}_\mathfrak{a}$ and heat supply $r_\mathfrak{a}$. In addition, to account for energy flux and energy supply associated with the time rate of change of volume distribution, a higher order stress and body force were introduced by Goodman & Cowin [11]. Such terms are expected since the volume distribution function and the motion are assumed to be kinematically independent. It is plausible, if a new independent quantity such as $\nu_\mathfrak{a}$ is introduced in a theory, a new equation must be introduced to determine its evolution. Following the approach of Goodman & Cowin [11] for dry granular materials, Passman et al. [23] choose to do this for a multiphase mixture also by means of an additional equation of balance for each constituent. According to [11] and [23], an equilibrated inertia $k_\mathfrak{a}$, equili-

brated stress vector $\boldsymbol{h}_\mathfrak{a}$, external equilibrated body force $l_\mathfrak{a}$[1] and intrinsic equilibrated body force $f_\mathfrak{a}$ are introduced for each constituent. Each distributed constituent must satisfy the basic laws of motion of continuum mechanics. We write the local equations of balance for each constituent $\mathfrak{a}$ ($\mathfrak{a} = 1, \ldots, N$) of the mixture in the following forms

– Conservation of mass

$$c_\mathfrak{a}^+ = \acute{\rho}_\mathfrak{a} + \rho_\mathfrak{a} \operatorname{div} \boldsymbol{v}_\mathfrak{a}, \tag{1}$$

– Balance of linear momentum

$$\boldsymbol{m}_\mathfrak{a}^+ = c_\mathfrak{a}^+ \boldsymbol{v}_\mathfrak{a} + \rho_\mathfrak{a} \acute{\boldsymbol{v}}_\mathfrak{a} - \operatorname{div} \boldsymbol{T}_\mathfrak{a} - \rho_\mathfrak{a} \boldsymbol{b}_\mathfrak{a}, \tag{2}$$

– Balance of angular momentum

$$\boldsymbol{M}_\mathfrak{a}^+ - \boldsymbol{r} \times \boldsymbol{m}_\mathfrak{a}^+ = \boldsymbol{T}_\mathfrak{a} - \boldsymbol{T}_\mathfrak{a}^T, \tag{3}$$

– Balance of equilibrated force

$$g_\mathfrak{a}^+ = c_\mathfrak{a}^+ k_\mathfrak{a} \acute{\nu}_\mathfrak{a} + \rho_\mathfrak{a} (k_\mathfrak{a} \acute{\nu}_\mathfrak{a})' - \operatorname{div} \boldsymbol{h}_\mathfrak{a} - \rho_\mathfrak{a} (l_\mathfrak{a} + f_\mathfrak{a}), \tag{4}$$

– Conservation of equilibrated inertia

$$\acute{k}_\mathfrak{a} = 0, \tag{5}$$

– Conservation of energy

$$\begin{aligned} e_\mathfrak{a}^+ = {} & c_\mathfrak{a}^+ \left(\varepsilon_\mathfrak{a} - \tfrac{1}{2} \boldsymbol{v}_\mathfrak{a} \cdot \boldsymbol{v}_\mathfrak{a} - \tfrac{1}{2} k_\mathfrak{a} \acute{\nu}_\mathfrak{a}^2 \right) + \boldsymbol{m}_\mathfrak{a}^+ \cdot \boldsymbol{v}_\mathfrak{a} \\ & + g_\mathfrak{a}^+ \acute{\nu}_\mathfrak{a} + \rho_\mathfrak{a} \acute{\varepsilon}_\mathfrak{a} - \boldsymbol{T}_\mathfrak{a} \cdot \boldsymbol{L}_\mathfrak{a} - \boldsymbol{h}_\mathfrak{a} \cdot \operatorname{grad} \acute{\nu}_\mathfrak{a} \\ & - \tfrac{1}{2} \rho_\mathfrak{a} \acute{k}_\mathfrak{a} \acute{\nu}_\mathfrak{a}^2 + \rho_\mathfrak{a} f_\mathfrak{a} \acute{\nu}_\mathfrak{a} + \operatorname{div} \boldsymbol{q}_\mathfrak{a} - \rho_\mathfrak{a} r_\mathfrak{a}, \end{aligned} \tag{6}$$

where $\acute{f}_\mathfrak{a} = \partial f / \partial t + (\operatorname{grad} f_\mathfrak{a}) \cdot \boldsymbol{v}_\mathfrak{a} = \dot{f}_\mathfrak{a} + (\operatorname{grad} f_\mathfrak{a}) \cdot \boldsymbol{u}_\mathfrak{a}$ is the material time derivative with respect to $\boldsymbol{v}_\mathfrak{a}$, $\dot{f}_\mathfrak{a} = \partial f / \partial t + (\operatorname{grad} f_\mathfrak{a}) \cdot \boldsymbol{v}$ the material time derivative with respect to the mixture velocity $\boldsymbol{v}$ and $\boldsymbol{u}_\mathfrak{a} = \boldsymbol{v}_\mathfrak{a} - \boldsymbol{v}$ the constituent diffusion velocity in the mixture; $\boldsymbol{r}$ is the position vector. $c_\mathfrak{a}^+$, $\boldsymbol{m}_\mathfrak{a}^+$, $\boldsymbol{M}_\mathfrak{a}^+$, $g_\mathfrak{a}^+$ and $e_\mathfrak{a}^+$ are, respectively, the internal growths (specific productions) of mass, linear momentum, angular momentum, equilibrated force and energy. A derivation of the equations of balance of equilibrated force and energy and the equation of conservation of equilibrated inertia can be found in references [11] and [23].

We require that the growths represent only exchanges among phases

$$\sum c_\mathfrak{a}^+ = 0, \ \sum \boldsymbol{m}_\mathfrak{a}^+ = \boldsymbol{0}, \ \sum \boldsymbol{M}_\mathfrak{a}^+ = \boldsymbol{0}, \ \sum g_\mathfrak{a}^+ = 0, \ \sum e_\mathfrak{a}^+ = 0. \tag{7}$$

Moreover, we assume that exchanges of mass and equilibrated force do not exist, although there is no particular difficulty in relaxing this assumption,

$$c_\mathfrak{a}^+ = 0, \ \ g_\mathfrak{a}^+ = 0, \tag{8}$$

and the exchange of angular momentum happens only through the exchange of linear momentum

$$\boldsymbol{M}_\mathfrak{a}^+ = \boldsymbol{r} \times \boldsymbol{m}_\mathfrak{a}^+. \tag{9}$$

[1] We do not see that, physically, such an external force can exist. We keep it here for formal coincidence with [11] and [23]. Our form of the second law does not depend on its existence.

Using these constraints (8) and (9), the equations of balance (1)–(6) can be rewritten in the forms

$$0 = \acute{\gamma}_\mathfrak{a} \nu_\mathfrak{a} + \acute{\nu}_\mathfrak{a} \gamma + \gamma_\mathfrak{a} \nu_\mathfrak{a} \operatorname{div} \boldsymbol{v}_\mathfrak{a}, \tag{10}$$

$$\boldsymbol{m}_\mathfrak{a}^+ = \rho_\mathfrak{a} \acute{\boldsymbol{v}}_\mathfrak{a} - \operatorname{div} \boldsymbol{T}_\mathfrak{a} - \rho_\mathfrak{a} \boldsymbol{b}_\mathfrak{a}, \tag{11}$$

$$\boldsymbol{0} = \boldsymbol{T}_\mathfrak{a} - \boldsymbol{T}_\mathfrak{a}^T, \tag{12}$$

$$0 = \rho_\mathfrak{a} k_\mathfrak{a} \acute{\nu}_\mathfrak{a} - \operatorname{div} \boldsymbol{h}_\mathfrak{a} - \rho_\mathfrak{a} (l_\mathfrak{a} + f_\mathfrak{a}), \tag{13}$$

$$\begin{aligned} e_\mathfrak{a}^+ = {} & \boldsymbol{m}_\mathfrak{a}^+ \cdot \boldsymbol{v}_\mathfrak{a} + \rho_\mathfrak{a} \acute{\varepsilon}_\mathfrak{a} - \boldsymbol{T}_\mathfrak{a} \cdot \boldsymbol{D}_\mathfrak{a} - \boldsymbol{h}_\mathfrak{a} \cdot \operatorname{grad} \acute{\nu}_\mathfrak{a} \\ & + \rho_\mathfrak{a} f_\mathfrak{a} \acute{\nu}_\mathfrak{a} + \operatorname{div} \boldsymbol{q}_\mathfrak{a} - \rho_\mathfrak{a} r_\mathfrak{a}. \end{aligned} \tag{14}$$

The summation of (14) for all constituents $\mathfrak{a}$ ($\mathfrak{a} = 1, 2, \ldots, N$) forms the balance equation of energy for the mixture as a whole equivalent to

$$\begin{aligned} 0 = {} & \rho \dot{\varepsilon} + \operatorname{div} \boldsymbol{q} - \boldsymbol{T} \cdot \boldsymbol{D} - \sum \boldsymbol{h}_\mathfrak{a} \cdot \operatorname{grad} \acute{\nu}_\mathfrak{a} \\ & + \sum \rho_\mathfrak{a} f_\mathfrak{a} \acute{\nu}_\mathfrak{a} - \rho r, \end{aligned} \tag{15}$$

where the constituent and mixtures fields are connected by the sum relations

$$\begin{aligned} & \rho = \sum \rho_\mathfrak{a}, \ \boldsymbol{v} = \sum \xi_\mathfrak{a} \boldsymbol{v}_\mathfrak{a}, \ \varepsilon = \varepsilon_I + \tfrac{1}{2} \sum \xi_\mathfrak{a} \boldsymbol{u}_\mathfrak{a} \cdot \boldsymbol{u}_\mathfrak{a}, \\ & \varepsilon_I = \sum \xi_\mathfrak{a} \varepsilon_\mathfrak{a}, \ r = \sum \xi_\mathfrak{a} r_\mathfrak{a} \end{aligned} \tag{16}$$

with $\sum = \sum_{\mathfrak{a}=1}^N$ and the constituent mass fraction

$$\xi_\mathfrak{a} = \rho_\mathfrak{a} / \rho. \tag{17}$$

As for the mixture fluxes, they take the usual forms As for the mixture fluxes, they take the usual forms

$$\begin{aligned} & \boldsymbol{T} = \sum \left(\boldsymbol{T}_\mathfrak{a} - \rho_\mathfrak{a} \boldsymbol{u}_\mathfrak{a} \otimes \boldsymbol{u}_\mathfrak{a} \right), \\ & \boldsymbol{q} = \sum \left\{ \boldsymbol{q}_\mathfrak{a} - \left[\boldsymbol{T}_\mathfrak{a} - \rho_\mathfrak{a} (\varepsilon_\mathfrak{a} + \tfrac{1}{2} \boldsymbol{u}_\mathfrak{a} \cdot \boldsymbol{u}_\mathfrak{a}) \boldsymbol{I} \right] \boldsymbol{u}_\mathfrak{a} \right\}. \end{aligned} \tag{18}$$

The balance laws (10)–(14) do not determine the field variables defined and interrelated by them uniquely. To that end some fields (here $\boldsymbol{T}_\mathfrak{a}$, $\boldsymbol{h}_\mathfrak{a}$, $f_\mathfrak{a}$, $\boldsymbol{q}_\mathfrak{a}$) must be expressed as functionals of the others, such that the emerging equations have the potential of generating well defined solutions. The forms of these constitutive relations are reduced or constained by the second law of thermodynamics which is here formulated as an entropy principle.

2.2 Entropy principle

There is an additive quantity for each constituent $\mathfrak{a}$, the entropy, with specific density $\eta_\mathfrak{a}$, flux $\boldsymbol{\phi}_\mathfrak{a}$, supply $s_\mathfrak{a}$ and growth of entropy $\eta_\mathfrak{a}^+$, for which we may write an equation of balance in the following local form

$$\eta_\mathfrak{a}^+ = \rho_\mathfrak{a} \acute{\eta}_\mathfrak{a} + \operatorname{div} (\boldsymbol{\phi}_\mathfrak{a}) - \rho_\mathfrak{a} s_\mathfrak{a}. \tag{19}$$

The summation of (19) over all constituents $\mathfrak{a}$ gives the equation of entropy balance for the mixture in the form

$$\Pi = \rho \dot{\eta} + \operatorname{div} \boldsymbol{\phi} - \rho s \tag{20}$$

where

$$\eta = \sum \xi_\mathfrak{a}\eta_\mathfrak{a}, \quad \boldsymbol{\phi} = \sum (\boldsymbol{\phi}_\mathfrak{a} + \rho_\mathfrak{a}\eta_\mathfrak{a}\boldsymbol{u}_\mathfrak{a}),$$
$$s = \sum \xi_\mathfrak{a} s_\mathfrak{a}, \quad \Pi = \sum \eta_\mathfrak{a}^+. \tag{21}$$

Following Truesdell [30], we do not restrict $\eta_\mathfrak{a}^+$ for each constituent except for the requirement that the total growth of entropy of the mixture be non-negative. Formally, this so-called second law of thermodynamics represents the restriction

$$\Pi = \rho\dot{\eta} + \operatorname{div}\boldsymbol{\phi} - \rho s \geq 0. \tag{22}$$

Now, any process, which satisfies (22), represents a so-called admissible process. Such a process, however, must in addition satisfy the balance relations (10)–(13) and (15) and other additional relations, if such relations should exist. One such constraint is that of saturation. It states that all constituents together fill the whole mixture space,

$$\sum \nu_\mathfrak{a} = 1. \tag{23}$$

We can also write this constraint condition as

$$\sum(\acute{\nu}_\mathfrak{a} - \boldsymbol{u}_\mathfrak{a} \cdot \operatorname{grad}\nu_\mathfrak{a}) = 0, \; t > 0 \quad \text{and}$$
$$\sum \nu_\mathfrak{a} = 1, \quad t = 0. \tag{24}$$

The second of these serves as an initial condition. In ensuing developments we further suppose that all constituents possess the same temperature θ. Such an assumption is tantamount to restricting considerations to the mixture energy equation rather than to each energy equation separately. We thus must satisfy the entropy inequality (22) subject to the simultaneous satisfaction of (10), (11), (13), (15) and (24). (The symmetry of the peculiar stress tensors is satisfied by postulating the constitutive relation accordingly). Liu [17] has shown that instead of fulfilling the entropy inequality for independent fields that are constrained by the balance laws and constraint conditions one may extend the entropy inequality by subtracting from it the products of each constraining equation with a Lagrange multiplier, viz.,

$$\begin{aligned}\Pi = {} & \rho\dot{\eta} + \operatorname{div}\boldsymbol{\phi} - \rho s \\ & - (1/\theta)\textstyle\sum \lambda_\mathfrak{a}^\nu [\acute{\gamma}_\mathfrak{a}\nu_\mathfrak{a} + \gamma_\mathfrak{a}\acute{\nu}_\mathfrak{a} + \gamma_\mathfrak{a}\nu_\mathfrak{a}\operatorname{div}\boldsymbol{v}_\mathfrak{a}] \\ & - (1/\theta)\textstyle\sum \boldsymbol{\lambda}_\mathfrak{a}^v \cdot [\rho_\mathfrak{a}\acute{\boldsymbol{v}}_\mathfrak{a} - \operatorname{div}\boldsymbol{T}_\mathfrak{a} - \rho_\mathfrak{a}\boldsymbol{b}_\mathfrak{a} - \boldsymbol{m}_\mathfrak{a}^+] \\ & - (1/\theta)\textstyle\sum \lambda_\mathfrak{a}^k [\rho_\mathfrak{a} k_\mathfrak{a}\acute{\nu}_\mathfrak{a} - \operatorname{div}\boldsymbol{h}_\mathfrak{a} - \rho_\mathfrak{a}(l_\mathfrak{a} + f_\mathfrak{a})] \\ & - \lambda^\varepsilon \big[\rho\dot{\varepsilon} + \operatorname{div}\boldsymbol{q} - \boldsymbol{T}\cdot\boldsymbol{D} - \textstyle\sum \boldsymbol{h}_\mathfrak{a} \cdot \operatorname{grad}\acute{\nu}_\mathfrak{a} + \sum \rho_\mathfrak{a} f_\mathfrak{a}\acute{\nu}_\mathfrak{a} \\ & \qquad - \rho r\big] - (\pi/\theta)\textstyle\sum[\acute{\nu}_\mathfrak{a} - \boldsymbol{u}_\mathfrak{a} \cdot \operatorname{grad}\nu_\mathfrak{a}] \geq 0, \end{aligned} \tag{25}$$

where $\lambda_\mathfrak{a}^\nu$, $\boldsymbol{\lambda}_\mathfrak{a}^v$, $\lambda_\mathfrak{a}^k$, λ^ε, π represent the corresponding Lagrange multipliers, and satisfying this extended inequality for unrestricted independent fields. (For convenience a factor $1/\theta$ has been extracted above from $\lambda_\mathfrak{a}^\nu$, $\boldsymbol{\lambda}_\mathfrak{a}^v$ $\lambda_\mathfrak{a}^k$ and π). These Lagrange multipliers may be constitutive quantities or independent variables. In the following evaluation of the entropy principle for a given constitutive class we can demonstrate that the Lagrange multipliers $\lambda_\mathfrak{a}^\nu$, $\boldsymbol{\lambda}_\mathfrak{a}^v$, $\lambda_\mathfrak{a}^k$ and λ^ε can be given by some constitutive relations, while on π no restriction is exerted, which therefore represents an independent variable.

Substituting the sum relations (16), (18) and (21) into (25) and introducing the mixture inner free energy

$$\psi_I = \sum \xi_\mathfrak{a}\psi_\mathfrak{a} = \varepsilon_I - \theta\eta \tag{26}$$

and the mixture flux density

$$\boldsymbol{j} = -\theta\boldsymbol{\phi} + \boldsymbol{q} = \boldsymbol{j}_c - \textstyle\sum \left(\boldsymbol{T}_\mathfrak{a} - \frac{\rho_\mathfrak{a}}{2}(\boldsymbol{u}_\mathfrak{a}\cdot\boldsymbol{u}_\mathfrak{a})\mathbf{1}\right)\boldsymbol{u}_\mathfrak{a} \tag{27}$$

with its constitutive part

$$\boldsymbol{j}_c := \textstyle\sum \boldsymbol{j}_\mathfrak{a} + \sum \rho_\mathfrak{a}\psi_\mathfrak{a}\boldsymbol{u}_\mathfrak{a} = \boldsymbol{j}_I + \sum \rho_\mathfrak{a}\psi_\mathfrak{a}\boldsymbol{u}_\mathfrak{a}, \tag{28}$$

where $\boldsymbol{j}_\mathfrak{a} = -\theta\boldsymbol{\phi}_\mathfrak{a} + \boldsymbol{q}_\mathfrak{a}$, yields the form

$$\begin{aligned}\theta\Pi = {} & -\rho(\dot{\psi}_I + \eta\dot{\theta}) - \textstyle\sum [\gamma_\mathfrak{a}\lambda_\mathfrak{a}^\nu + \pi + \rho_\mathfrak{a} f_\mathfrak{a}]\acute{\nu}_\mathfrak{a} \\ & - \textstyle\sum \rho_\mathfrak{a}(\boldsymbol{\lambda}_\mathfrak{a}^v + \boldsymbol{u}_\mathfrak{a})\cdot\acute{\boldsymbol{v}}_\mathfrak{a} - \boldsymbol{\phi}\cdot\operatorname{grad}\theta - \operatorname{div}\boldsymbol{j}_c \\ & + \textstyle\sum (\boldsymbol{\lambda}_\mathfrak{a}^v + \boldsymbol{u}_\mathfrak{a})\cdot\operatorname{div}\boldsymbol{T}_\mathfrak{a} + \sum (\boldsymbol{T}_\mathfrak{a} - \gamma_\mathfrak{a}\nu_\mathfrak{a}\lambda_\mathfrak{a}^\nu\boldsymbol{I})\cdot\boldsymbol{D}_\mathfrak{a} \\ & - \textstyle\sum \lambda_\mathfrak{a}^k\rho_\mathfrak{a}k_\mathfrak{a}\acute{\nu}_\mathfrak{a} + \sum \lambda_\mathfrak{a}^k \operatorname{div}\boldsymbol{h}_\mathfrak{a} + \sum \lambda_\mathfrak{a}^k\rho_\mathfrak{a}f_\mathfrak{a} \\ & - \textstyle\sum \lambda_\mathfrak{a}^\nu\nu_\mathfrak{a}\acute{\gamma}_\mathfrak{a} + \sum \boldsymbol{\lambda}_\mathfrak{a}^v\cdot\boldsymbol{m}_\mathfrak{a}^+ + \sum \boldsymbol{h}_\mathfrak{a}\cdot\operatorname{grad}\acute{\nu}_\mathfrak{a} \\ & + \textstyle\sum \pi\boldsymbol{u}_\mathfrak{a}\cdot\operatorname{grad}\nu_\mathfrak{a} \geq 0 \end{aligned} \tag{29}$$

of the entropy inequality with the assumption $\lambda^\varepsilon = 1/\theta$. This assumption is not reasonable in cases when $\dot{\theta}$ should also be an independent constitutive variable. As we will not include such a dependence the a priori assignment $\lambda^\varepsilon = 1/\theta$ is justifiable on the basis that Müller & Liu have proved it in [18] and Svendsen & Hutter could also show it in the context of [19], but did not publish the result. For single fluids or mixtures of fluids, this assumption can be directly obtained from the evaluation of the entropy inequality by use of the property of the entropy that on an ideal wall where the entropy production vanishes the normal component of the entropy flux is continuous (see e.g. [18]). In deducing (29), we assumed also that the material behaviour is independent of the supplies, i.e., that all external source terms balance, viz.,

$$\theta\rho s - \textstyle\sum \boldsymbol{\lambda}_\mathfrak{a}^v\cdot\rho_\mathfrak{a}\boldsymbol{b}_\mathfrak{a} - \sum \lambda_\mathfrak{a}^k\rho_\mathfrak{a}l_\mathfrak{a} - \rho r = 0. \tag{30}$$

This form of the entropy inequality (29) will be used to investigate the constitutive postulates in the next section.

3
Constitutive principles

We recall that the purpose of the entropy principle is to derive restrictions upon the constitutive relations. The entropy and its flux as well as the Lagrange multipliers must be considered as auxiliary quantities. In this section we evaluate the entropy inequality (29) for a given constitutive class, which is suitable for a fluid-granular mixture.

3.1
Constitutive equations

We write constitutive equations in which for each constituent $\mathfrak{a}$, the material specific dependent variables

$$\mathcal{C}_\mathfrak{a} := \{\psi_\mathfrak{a},\ \eta_\mathfrak{a},\ \boldsymbol{T}_\mathfrak{a},\ \boldsymbol{h}_\mathfrak{a},\ \boldsymbol{q}_\mathfrak{a},\ \boldsymbol{\phi}_\mathfrak{a}\} \tag{31}$$

are functionals only of variables of the same constituent $\mathfrak{a}$ (principle of phase separation). We suppose here that these independent variables are

$$\mathcal{S}_\mathfrak{a} := (\nu_\mathfrak{a},\ \operatorname{grad}\nu_\mathfrak{a}, \acute{\nu}_\mathfrak{a}, \gamma_\mathfrak{a},\ \operatorname{grad}\gamma_\mathfrak{a}, \theta,\ \operatorname{grad}\theta, \boldsymbol{D}_\mathfrak{a}). \tag{32}$$

Quite naturally, the growths $\boldsymbol{m}_\mathfrak{a}^+$ may depend on the independent variables of all constituents, here chosen in the form $\mathcal{F}_\mathfrak{b},\ \mathfrak{b} = 1, 2, \ldots, N$,

$$\mathcal{F}_\mathfrak{b} = (\nu_\mathfrak{b},\ \operatorname{grad}\nu_\mathfrak{b}, \acute{\nu}_\mathfrak{b}, \gamma_\mathfrak{b},\ \operatorname{grad}\gamma_\mathfrak{b}, \theta,\ \operatorname{grad}\theta, \boldsymbol{D}_\mathfrak{b}, \boldsymbol{u}_\mathfrak{b}, \boldsymbol{\mathcal{W}}_\mathfrak{b}), \tag{33}$$

where $\boldsymbol{D}_\mathfrak{a}$ is the symmetric part, and $\boldsymbol{W}_\mathfrak{a}$ the skew-symmetric part of $\operatorname{grad}\boldsymbol{v}_\mathfrak{a}$, representing corresponding deformation rate and vorticity tensors, respectively; $\boldsymbol{\mathcal{W}}_\mathfrak{a}$ represents the difference

$$\boldsymbol{\mathcal{W}}_\mathfrak{a} = \boldsymbol{W}_\mathfrak{a} - \boldsymbol{W}, \tag{34}$$

where $\boldsymbol{W} = \operatorname{skw}(\operatorname{grad}\boldsymbol{v})$. To conform with the principle of material objectivity (material frame indifference) the constitutive quantities cannot depend on all velocities of constituents $\boldsymbol{v}_\mathfrak{a}$ and the skew-symmetric parts of their gradients (except for the symmetric parts), only on the relative velocities $\boldsymbol{u}_\mathfrak{a} = \boldsymbol{v}_\mathfrak{a} - \boldsymbol{v}$ (constituent diffusion velocities) and the corresponding gradients. In short,

$$\left.\begin{aligned} &\mathcal{C}_\mathfrak{a} = \hat{\mathcal{C}}_\mathfrak{a}(\mathcal{S}_\mathfrak{a}),\\ &\boldsymbol{m}_\mathfrak{a}^+ = \hat{\boldsymbol{m}}_\mathfrak{a}^+(\mathcal{F}_\mathfrak{b},\ \mathfrak{b} = 1, \ldots, N), \end{aligned}\right\} (\mathfrak{a} = 1, \ldots, N). \tag{35}$$

Strictly speaking, according to the principle of equipresence [29] in Truesdell's original list, all the dependent constitutive variables must be functions of all the independent constitutive variables. However, for simplicity of calculation, we have replaced the principle of equipresence by the priciple of phase separation, which has been adopted in many mixture theories (e.g. [1, 23]). Practically, in multiphase mixtures, the individual constituents are clearly separated physically and it is plausible to think of the mixture as phase separated. On the other hand we ought to mention that there are also valid plausibility arguments to reject the principle of phase separation, since the different constituents in the mixture may appear as different materials in combination with the other constituents than without. A theory which imposes the principle of equipresence is far more complicated, and inferences from the entropy principle are far more difficult to draw. At last, only the results in concrete situations can decide whether the simple theory will be meaningful.

These constitutive equations must satisfy the entropy inequality (29). Substituting the constitutive relations (31)–(33) into (29), and using the identities

$$\begin{aligned} &\dot{\nu}_\mathfrak{a} = \acute{\nu}_\mathfrak{a} - \operatorname{grad}\nu_\mathfrak{a}\cdot\boldsymbol{u}_\mathfrak{a},\ \ \dot{\acute{\nu}}_\mathfrak{a} = \ddot{\nu}_\mathfrak{a} - \operatorname{grad}\acute{\nu}_\mathfrak{a}\cdot\boldsymbol{u}_\mathfrak{a},\\ &\dot{\gamma}_\mathfrak{a} = \acute{\gamma}_\mathfrak{a} - \operatorname{grad}\gamma_\mathfrak{a}\cdot\boldsymbol{u}_\mathfrak{a},\\ &\dot{\overline{\operatorname{grad}\nu_\mathfrak{a}}} = \operatorname{grad}\acute{\nu}_\mathfrak{a} - \operatorname{grad}\nu_\mathfrak{a}\operatorname{grad}\boldsymbol{v}_\mathfrak{a} - \operatorname{grad}(\operatorname{grad}\nu_\mathfrak{a})\cdot\boldsymbol{u}_\mathfrak{a}, \end{aligned} \tag{36}$$

yields the new inequality

$$\begin{aligned} \theta\Pi = &-\rho\left[\frac{\partial\psi_I}{\partial\theta} + \eta\right]\dot{\theta} - \rho\frac{\partial\psi_I}{\partial\operatorname{grad}\theta}\cdot\dot{\overline{\operatorname{grad}\theta}} - \sum\rho\frac{\partial\psi_I}{\partial\boldsymbol{D}_\mathfrak{a}}\cdot\dot{\boldsymbol{D}}_\mathfrak{a}\\ &-\sum\left[\rho\frac{\partial\psi_I}{\partial\gamma_\mathfrak{a}} + \lambda_\mathfrak{a}^\nu\nu_\mathfrak{a}\right]\acute{\gamma}_\mathfrak{a} - \sum\left[\rho\frac{\partial\psi_I}{\partial\acute{\nu}_\mathfrak{a}} + \lambda_\mathfrak{a}^k\rho_\mathfrak{a}k_\mathfrak{a}\right]\ddot{\nu}_\mathfrak{a}\\ &-\sum\left[\rho\frac{\partial\psi_I}{\partial\nu_\mathfrak{a}} + \gamma_\mathfrak{a}\lambda_\mathfrak{a}^\nu + \rho_\mathfrak{a}f_\mathfrak{a} + \pi\right]\acute{\nu}_\mathfrak{a}\\ &+\sum\left[\rho\frac{\partial\psi_I}{\partial\gamma_\mathfrak{a}}\boldsymbol{u}_\mathfrak{a} - \frac{\partial\boldsymbol{j}_c}{\partial\gamma_\mathfrak{a}}\right]\cdot\operatorname{grad}\gamma_a\\ &+\sum\left[\rho\frac{\partial\psi_I}{\partial\nu_\mathfrak{a}}\boldsymbol{u}_\mathfrak{a} + \pi\boldsymbol{u}_\mathfrak{a} - \frac{\partial\boldsymbol{j}_c}{\partial\nu_\mathfrak{a}}\right]\cdot\operatorname{grad}\nu_\mathfrak{a}\\ &-\sum\left[\rho\frac{\partial\psi_I}{\partial\operatorname{grad}\nu_\mathfrak{a}} + \rho\frac{\partial\psi_I}{\partial\acute{\nu}_\mathfrak{a}}\boldsymbol{u}_\mathfrak{a} - \frac{\partial\boldsymbol{j}_c}{\partial\acute{\nu}_\mathfrak{a}} - \boldsymbol{h}_\mathfrak{a}\right]\cdot\operatorname{grad}\acute{\nu}_\mathfrak{a}\\ &+\sum\rho\frac{\partial\psi_I}{\partial\operatorname{grad}\gamma_\mathfrak{a}}\cdot\dot{\overline{\operatorname{grad}\gamma_\mathfrak{a}}} - \sum\frac{\partial\boldsymbol{j}_c}{\partial\operatorname{grad}\gamma_\mathfrak{a}}\cdot\operatorname{grad}\operatorname{grad}\gamma_\mathfrak{a}\\ &+\sum\left[\boldsymbol{T}_\mathfrak{a} - \gamma_\mathfrak{a}\nu_\mathfrak{a}\lambda_\mathfrak{a}^\nu\boldsymbol{I} + \rho\frac{\partial\psi_I}{\partial\operatorname{grad}\nu_\mathfrak{a}}\otimes\operatorname{grad}\nu_\mathfrak{a} - \frac{\partial\boldsymbol{j}_c}{\partial\boldsymbol{v}_\mathfrak{a}}\right]\cdot\boldsymbol{D}_\mathfrak{a}\\ &+\sum\left[\rho\frac{\partial\psi_I}{\partial\operatorname{grad}\nu_\mathfrak{a}}\otimes\operatorname{grad}\nu_\mathfrak{a} - \frac{\partial\boldsymbol{j}_c}{\partial\boldsymbol{v}_\mathfrak{a}}\right]\cdot\boldsymbol{W}_\mathfrak{a}\\ &-\left[\boldsymbol{\phi} + \frac{\partial\boldsymbol{j}_c}{\partial\theta}\right]\cdot\operatorname{grad}\theta\\ &+\sum\left[-\frac{\partial\boldsymbol{j}_c}{\partial\operatorname{grad}\nu_\mathfrak{a}} + \rho\frac{\partial\psi_I}{\partial\operatorname{grad}\nu_\mathfrak{a}}\otimes\boldsymbol{u}_\mathfrak{a}\right]\cdot\operatorname{grad}(\operatorname{grad}\nu_\mathfrak{a})\\ &-\frac{\partial\boldsymbol{j}_c}{\partial\operatorname{grad}\theta}\cdot\operatorname{grad}(\operatorname{grad}\theta) - \sum\frac{\partial\boldsymbol{j}_c}{\partial\boldsymbol{D}_\mathfrak{a}}\cdot\operatorname{grad}\boldsymbol{D}_\mathfrak{a}\\ &-\sum\rho_\mathfrak{a}(\boldsymbol{\lambda}_\mathfrak{a}^v + \boldsymbol{u}_\mathfrak{a})\cdot\dot{\boldsymbol{v}}_\mathfrak{a} + \sum(\boldsymbol{\lambda}_\mathfrak{a}^v + \boldsymbol{u}_\mathfrak{a})\cdot\operatorname{div}\boldsymbol{T}_\mathfrak{a}\\ &+\sum\boldsymbol{\lambda}_\mathfrak{a}^v\cdot\boldsymbol{m}_\mathfrak{a}^+ + \sum\lambda_\mathfrak{a}^k\rho_\mathfrak{a}f_\mathfrak{a} + \sum\lambda_\mathfrak{a}^k\operatorname{div}\boldsymbol{h}_\mathfrak{a} \geq 0. \end{aligned} \tag{37}$$

It possesses the form

$$\boldsymbol{a}\cdot\boldsymbol{\alpha} + b \geq 0, \tag{38}$$

where the vector $\boldsymbol{a}$ and the scalar b are functions of the variables listed in (32) and (33), and the vector $\boldsymbol{\alpha}$ depends on time and space derivatives of these quantities. Hence inequality (38) is linear in $\boldsymbol{\alpha}$, and since these variables can take any values, it would be able to violate (38) unless

$$\boldsymbol{a} = \boldsymbol{0} \text{ and } b \geq 0. \tag{39}$$

Explicitly, the entropy inequality must hold for all independent variations of $\boldsymbol{\alpha} = \{\dot{\theta},\ \dot{\overline{\operatorname{grad}\theta}},\ \dot{\boldsymbol{D}}_\mathfrak{a},\ \acute{\gamma}_\mathfrak{a},\ \dot{\boldsymbol{v}}_\mathfrak{a},\ \ddot{\nu}_\mathfrak{a},\ \operatorname{grad}\acute{\nu}_\mathfrak{a},\ \dot{\overline{\operatorname{grad}\gamma_\mathfrak{a}}},\ \operatorname{grad}(\operatorname{grad}\gamma_\mathfrak{a}),\ \operatorname{grad}(\operatorname{grad}\nu_\mathfrak{a}),\ \operatorname{grad}(\operatorname{grad}\theta)$ and $\operatorname{grad}\boldsymbol{D}_\mathfrak{a}\}$. These variables appear linearly

in the inequality (37) and thus their coefficients must vanish. It then follows that the expressions for the Lagrange multipliers $\boldsymbol{\lambda}^v_{\mathfrak{a}}$, $\lambda^\nu_{\mathfrak{a}}$, $\lambda^k_{\mathfrak{a}}$ are given by

$$\boldsymbol{\lambda}^v_{\mathfrak{a}} = -\boldsymbol{u}_{\mathfrak{a}}, \tag{40}$$

$$\lambda^k_{\mathfrak{a}} = -\frac{\rho}{\rho_{\mathfrak{a}} k_{\mathfrak{a}}}\frac{\partial \psi_I}{\partial \acute{\nu}_{\mathfrak{a}}} = -\frac{1}{k_{\mathfrak{a}}}\frac{\partial \psi_{\mathfrak{a}}}{\partial \acute{\nu}_{\mathfrak{a}}}, \tag{41}$$

$$\lambda^\nu_{\mathfrak{a}} = -\frac{\rho}{\nu_{\mathfrak{a}}}\frac{\partial \psi_I}{\partial \gamma_{\mathfrak{a}}} = -\gamma_{\mathfrak{a}}\frac{\partial \psi_{\mathfrak{a}}}{\partial \gamma_{\mathfrak{a}}}. \tag{42}$$

To simplify our problem, we will now assume that the free energy $\psi_{\mathfrak{a}}$ is independent of $\acute{\nu}_{\mathfrak{a}}$, so the Lagrange multiplier $\lambda^k_{\mathfrak{a}}$ must vanish,

$$\lambda^k_{\mathfrak{a}} = 0. \tag{43}$$

The entropy inequality (37) implies also the following restrictions for the constitutive variables

$$\eta = -\frac{\partial \psi_I}{\partial \theta}, \tag{44}$$

$$\frac{\partial \psi_I}{\partial \operatorname{grad}\theta} = \mathbf{0}, \quad \frac{\partial \psi_I}{\partial \boldsymbol{D}_{\mathfrak{a}}} = \mathbf{0}, \quad \frac{\partial \psi_I}{\partial \operatorname{grad}\gamma_{\mathfrak{a}}} = \mathbf{0}, \tag{45}$$

$$\boldsymbol{h}_{\mathfrak{a}} = -\rho\frac{\partial \psi_I}{\partial \operatorname{grad}\nu_{\mathfrak{a}}} - \rho\frac{\partial \psi_I}{\partial \acute{\nu}_{\mathfrak{a}}}\boldsymbol{u}_{\mathfrak{a}} + \frac{\partial \boldsymbol{j}_c}{\partial \acute{\nu}_{\mathfrak{a}}}, \tag{46}$$

$$\frac{\partial \boldsymbol{j}_c}{\partial \operatorname{grad}\theta} \cdot \operatorname{grad}(\operatorname{grad}\theta) = 0, \tag{47}$$

$$\frac{\partial \boldsymbol{j}_c}{\partial \operatorname{grad}\gamma_{\mathfrak{a}}} \cdot \operatorname{grad}(\operatorname{grad}\gamma_{\mathfrak{a}}) = 0, \tag{48}$$

$$\left(\rho\frac{\partial \psi_I}{\partial \operatorname{grad}\nu_{\mathfrak{a}}} \otimes \boldsymbol{u}_{\mathfrak{a}} - \frac{\partial \boldsymbol{j}_c}{\partial \operatorname{grad}\nu_{\mathfrak{a}}}\right) \cdot \operatorname{grad}(\operatorname{grad}\nu_{\mathfrak{a}}) = 0, \tag{49}$$

$$\frac{\partial \boldsymbol{j}_c}{\partial \boldsymbol{D}_{\mathfrak{a}}} \cdot \operatorname{grad}\boldsymbol{D}_{\mathfrak{a}} = 0. \tag{50}$$

Eqs. (40)–(50) correspond to $\boldsymbol{a} = \mathbf{0}$ in (39).

The restrictions (45) on the form of the mixture specific inner free energy yield

$$\begin{aligned}&\psi_I = \hat{\psi}_I(\nu_1, \ldots, \nu_N, \operatorname{grad}\nu_1, \ldots, \operatorname{grad}\nu_N, \gamma_1, \ldots, \gamma_N, \theta)\\ &\implies \psi_{\mathfrak{a}} = \hat{\psi}_{\mathfrak{a}}(\nu_{\mathfrak{a}}, \operatorname{grad}\nu_{\mathfrak{a}}, \gamma_{\mathfrak{a}}, \theta).\end{aligned} \tag{51}$$

Using (28) and (51), one can rewrite the restrictions (47)–(49) on $\boldsymbol{j}_c$ into the restrictions on its inner parts $\boldsymbol{j}_I$ in the forms

$$\frac{\partial \boldsymbol{j}_I}{\partial \operatorname{grad}\theta} \cdot \operatorname{grad}(\operatorname{grad}\theta) = 0, \tag{52}$$

$$\frac{\partial \boldsymbol{j}_I}{\partial \operatorname{grad}\gamma_{\mathfrak{a}}} \cdot \operatorname{grad}(\operatorname{grad}\gamma_{\mathfrak{a}}) = 0, \tag{53}$$

$$\frac{\partial \boldsymbol{j}_I}{\partial \operatorname{grad}\nu_{\mathfrak{a}}} \cdot \operatorname{grad}(\operatorname{grad}\nu_{\mathfrak{a}}) = 0. \tag{54}$$

These three restrictions mean that $\partial \boldsymbol{j}_I/\partial \operatorname{grad}\theta$, $\partial \boldsymbol{j}_I/\partial \operatorname{grad}\gamma_{\mathfrak{a}}$ and $\partial \boldsymbol{j}_I/\partial \operatorname{grad}\nu_{\mathfrak{a}}$ are skew-symmetric, which implies that $\boldsymbol{j}_I$ are collinear to $\operatorname{grad}\theta$, $\operatorname{grad}\gamma_{\mathfrak{a}}$ and $\operatorname{grad}\nu_{\mathfrak{a}}$, with the corresponding material coefficient tensors being skew-symmetric. On the other hand, the isotropy of $\boldsymbol{j}_I$ requires any such material tensors to be symmetric. To satisfy both requirements requires then, these tensors must vanish, making $\boldsymbol{j}_I$ independent of $\operatorname{grad}\theta$, $\operatorname{grad}\gamma_{\mathfrak{a}}$ and $\operatorname{grad}\nu_{\mathfrak{a}}$, and yielding its reduced form

$$\begin{aligned}&\boldsymbol{j}_I = \hat{\boldsymbol{j}}_I(\theta, \nu_1, \ldots, \nu_N, \acute{\nu}_1, \ldots, \acute{\nu}_N, \gamma_1, \ldots, \gamma_N, \theta,\\ &\qquad\qquad \boldsymbol{D}_1, \ldots, \boldsymbol{D}_N)\\ &\text{or}\quad \boldsymbol{j}_{\mathfrak{a}} = \hat{\boldsymbol{j}}_{\mathfrak{a}}(\theta, \nu_{\mathfrak{a}}, \acute{\nu}_{\mathfrak{a}}, \gamma_{\mathfrak{a}}, \boldsymbol{D}_{\mathfrak{a}}).\end{aligned} \tag{55}$$

If we restrict attention to isotropic behaviour, the special form (55) necessarily implies $\boldsymbol{j}_{\mathfrak{a}} = \mathbf{0}$, $\forall \mathfrak{a}$, (there is no isotropic vectorial function of only scalars and a second rank tensor) and thus, the constituent entropy fluxes are equal to constituent heat fluxes divided by absolute temperature (see eq. after (28)),

$$\boldsymbol{\phi}_{\mathfrak{a}} = \boldsymbol{q}_{\mathfrak{a}}/\theta, \tag{56}$$

which in the entropy principle of Coleman-Noll are from the outset assumed, and

$$\boldsymbol{j}_I = \mathbf{0}. \tag{57}$$

In this case, $\boldsymbol{j}_c$ reduces to

$$\boldsymbol{j}_c = \sum \rho_{\mathfrak{a}}\psi_{\mathfrak{a}}\boldsymbol{u}_{\mathfrak{a}}. \tag{58}$$

Let $\psi_{\mathfrak{a}}$ be an isotropic function; then (51) implies

$$\psi_{\mathfrak{a}} = \hat{\psi}_{\mathfrak{a}}(\nu_{\mathfrak{a}}, \operatorname{grad}\nu_{\mathfrak{a}} \cdot \operatorname{grad}\nu_{\mathfrak{a}}, \gamma_{\mathfrak{a}}, \theta). \tag{59}$$

Substituting (59) and (58) into (46) asserts that the equilibrated stress $\boldsymbol{h}_{\mathfrak{a}}$ has the representation

$$\boldsymbol{h}_{\mathfrak{a}} = \rho_{\mathfrak{a}}\frac{\partial \psi_{\mathfrak{a}}}{\partial \operatorname{grad}\nu_{\mathfrak{a}}} = \mathcal{A}_{\mathfrak{a}} \operatorname{grad}\nu_{\mathfrak{a}}, \tag{60}$$

where

$$\mathcal{A}_{\mathfrak{a}} = \hat{\mathcal{A}}_{\mathfrak{a}}(\nu_{\mathfrak{a}}, \operatorname{grad}\nu_{\mathfrak{a}}, \gamma_{\mathfrak{a}}, \theta) = 2\rho_{\mathfrak{a}}\frac{\partial \psi_{\mathfrak{a}}}{\partial(\operatorname{grad}\nu_{\mathfrak{a}} \cdot \operatorname{grad}\nu_{\mathfrak{a}})}. \tag{61}$$

According to (58) and (60), we can obtain that

$$\left[\rho\frac{\partial \psi_I}{\partial \operatorname{grad}\nu_{\mathfrak{a}}} \otimes \operatorname{grad}\nu_{\mathfrak{a}} - \frac{\partial \boldsymbol{j}_c}{\partial \boldsymbol{v}_{\mathfrak{a}}}\right] \cdot \boldsymbol{W}_{\mathfrak{a}} = 0, \tag{62}$$

since the bracketed term is symmetric whereas $\boldsymbol{W}_{\mathfrak{a}}$ is skew-symmetric. Returning now to the entropy inequality (37) and employing these restrictions, and the identities from (58)

$$\begin{aligned}\frac{\partial \boldsymbol{j}_c}{\partial \boldsymbol{v}_{\mathfrak{a}}} &= \rho_{\mathfrak{a}}(\psi_{\mathfrak{a}} - \psi_I)\boldsymbol{I},\\ \frac{\partial \boldsymbol{j}_c}{\partial \nu_{\mathfrak{a}}} &= \gamma_{\mathfrak{a}}(\psi_{\mathfrak{a}} - \psi_I)\boldsymbol{u}_{\mathfrak{a}} + \rho_{\mathfrak{a}}\frac{\partial \psi_{\mathfrak{a}}}{\partial \nu_{\mathfrak{a}}}\boldsymbol{u}_{\mathfrak{a}},\\ \frac{\partial \boldsymbol{j}_c}{\partial \gamma_{\mathfrak{a}}} &= \nu_{\mathfrak{a}}(\psi_{\mathfrak{a}} - \psi_I)\boldsymbol{u}_{\mathfrak{a}} + \rho_{\mathfrak{a}}\frac{\partial \psi_{\mathfrak{a}}}{\partial \gamma_{\mathfrak{a}}}\boldsymbol{u}_{\mathfrak{a}},\end{aligned}$$

we obtain the reduced entropy inequality

$$\begin{aligned}\theta\Pi = &-\sum\left[\beta_\mathfrak{a} - p_\mathfrak{a} + \gamma_\mathfrak{a}\nu_\mathfrak{a} f_\mathfrak{a} + \pi\right]\dot{\nu}_\mathfrak{a} \\ &+\sum\left[\left(\gamma_\mathfrak{a}(\psi_I - \psi_\mathfrak{a}) + \pi\right)\operatorname{grad}\nu_\mathfrak{a}\right. \\ &\qquad \left.+\nu_\mathfrak{a}(\psi_I - \psi_\mathfrak{a})\operatorname{grad}\gamma_\mathfrak{a}\right]\cdot\boldsymbol{u}_\mathfrak{a} - \sum \boldsymbol{m}_\mathfrak{a}^{+}\cdot\boldsymbol{v}_\mathfrak{a} \\ &+\sum\left[\boldsymbol{T}_\mathfrak{a} + \nu_\mathfrak{a}\left(p_\mathfrak{a} + \gamma_\mathfrak{a}(\psi_I - \psi_\mathfrak{a})\right)\boldsymbol{I}\right. \\ &\qquad \left.+\mathcal{A}_\mathfrak{a}\operatorname{grad}\nu_\mathfrak{a}\otimes\operatorname{grad}\nu_\mathfrak{a}\right]\cdot\boldsymbol{D}_\mathfrak{a} \\ &-\left[\boldsymbol{\phi} + \frac{\partial \boldsymbol{j}_c}{\partial\theta}\right]\cdot\operatorname{grad}\theta \geq 0, \end{aligned} \tag{63}$$

where $p_\mathfrak{a}$ is the *thermodynamic pressure*

$$p_\mathfrak{a} := \gamma_\mathfrak{a}^2\frac{\partial\psi_\mathfrak{a}}{\partial\gamma_\mathfrak{a}} \tag{64}$$

and $\beta_\mathfrak{a}$ is the *configuration pressure*

$$\beta_\mathfrak{a} := \rho_\mathfrak{a}\frac{\partial\psi_\mathfrak{a}}{\partial\nu_\mathfrak{a}}. \tag{65}$$

The inequality (63) corresponds to $b \geq 0$ in (39).

At this point we should also point out that the constitutive class (32), (33) is suitable for mixtures with compressible constituents. For density preserving constituents, i.e. constituents whose true mass density does not change, $\gamma_\mathfrak{a}$ and $\operatorname{grad}\gamma_\mathfrak{a}$ are no longer independent variables. In this case returning to the initial constitutive assumption (32), (33), we delete the dependences on $\gamma_\mathfrak{a}$ and $\operatorname{grad}\gamma_\mathfrak{a}$ from the constitutive equations and repeat the above analysis. We find the same constitutive restrictions for mixtures with density preserving constituents as before for compressible constituents, if here $p_\mathfrak{a} = -\gamma_\mathfrak{a}\lambda_\mathfrak{a}^\nu$ is introduced, which now is an unknown variable and can no longer be determined by the free energy $\psi_\mathfrak{a}$ as expressed in (64). We shall not repeat the details of the analysis. We further should point that inequality (63) looks as if entropy would be produced by the saturation pressure π by the terms in the first and second lines on the RHS of (63). However this is not so, because π only contributes to the equilibrium parts of the constitutive quantities $f_\mathfrak{a}$ and $\boldsymbol{m}_\mathfrak{a}^{+}$, while the residual dissipation inequality depends only on non-equilibrium parts of these quantities as we shall demonstrate shortly.

3.2 Thermodynamic equilibrium

As usual, further restrictions on the constitutive relations can be obtained from the residual inequality (63) in the context of thermodynamic equilibrium, which is characterized by the vanishing of the entropy production rate density Π. In the context of the current constitutive class, Π vanishes when the independent dynamic variables

$$\boldsymbol{Y} = (\dot{\nu}_1, \ldots, \dot{\nu}_N, \operatorname{grad}\theta, \boldsymbol{v}_1, \ldots, \boldsymbol{v}_N, \boldsymbol{D}_1, \ldots, \boldsymbol{D}_N) \tag{66}$$

all vanish, which implies that Π assumes its minimum, zero, in thermodynamic equilibrium. Necessary conditions for this minimum are that

$$\begin{aligned}&\frac{\partial\Pi}{\partial Y_i}\Big|_{\boldsymbol{Y}=\boldsymbol{0}} = 0, && Y_i \in \boldsymbol{Y}, \\ &\frac{\partial^2\Pi}{\partial Y_i\,\partial Y_j}\Big|_{\boldsymbol{Y}=\boldsymbol{0}} \text{ is non-negative definite, } && Y_i,\, Y_j \in \boldsymbol{Y}. \end{aligned} \tag{67}$$

As is well-known, the first condition restricts the equilibrium forms of the dependent constitutive fields, while the second constrains the signs of certain material parameters; here we deal only with the first:

$$\begin{aligned}&\frac{\partial\Pi}{\partial\dot{\nu}_\mathfrak{a}}\Big|_{\boldsymbol{Y}=\boldsymbol{0}} = \boldsymbol{0},\ \frac{\partial\Pi}{\partial\operatorname{grad}\theta}\Big|_{\boldsymbol{Y}=\boldsymbol{0}} = \boldsymbol{0}, \\ &\frac{\partial\Pi}{\partial\boldsymbol{v}_\mathfrak{a}}\Big|_{\boldsymbol{Y}=\boldsymbol{0}} = \boldsymbol{0},\ \frac{\partial\Pi}{\partial\boldsymbol{D}_\mathfrak{a}}\Big|_{\boldsymbol{Y}=\boldsymbol{0}} = \boldsymbol{0}. \end{aligned} \tag{68}$$

These restrictions yield the following expressions for the equilibrated internal force $f_\mathfrak{a}$, the entropy flux $\boldsymbol{\phi}$, the heat flux $\boldsymbol{q}$, the stress $\boldsymbol{T}_\mathfrak{a}$ and the momentum exchange rate density $\boldsymbol{m}_\mathfrak{a}^{+}$ in thermodynamic equilibrium (denoted by the superscript E)

$$f_\mathfrak{a}^E = \frac{p_\mathfrak{a} - \beta_\mathfrak{a}}{\gamma_\mathfrak{a}\nu_\mathfrak{a}} - \frac{\pi}{\gamma_\mathfrak{a}\nu_\mathfrak{a}}, \tag{69}$$

$$\boldsymbol{\phi}^E = \boldsymbol{0}, \tag{70}$$

$$\boldsymbol{q}^E = \boldsymbol{0}, \tag{71}$$

$$\boldsymbol{T}_\mathfrak{a}^E = -\nu_\mathfrak{a}\left(p_\mathfrak{a} + \gamma_\mathfrak{a}(\psi_I - \psi_\mathfrak{a})\right)\boldsymbol{I} - \mathcal{A}_\mathfrak{a}\operatorname{grad}\nu_\mathfrak{a}\otimes\operatorname{grad}\nu_\mathfrak{a}, \tag{72}$$

$$\begin{aligned}\boldsymbol{m}_\mathfrak{a}^{+E} &= \textstyle\sum_\mathfrak{b}\left\{\left[\pi + \gamma_\mathfrak{b}(\psi_I - \psi_\mathfrak{b})\right]\operatorname{grad}\nu_\mathfrak{b}\right. \\ &\qquad \left.+\nu_\mathfrak{b}(\psi_I - \psi_\mathfrak{b})\operatorname{grad}\gamma_\mathfrak{b}\right\}(\delta_{\mathfrak{a}\mathfrak{b}} - \xi_\mathfrak{a}) \\ &= \pi\operatorname{grad}\nu_\mathfrak{a} + \textstyle\sum_\mathfrak{b}(\psi_I - \psi_\mathfrak{b})\operatorname{grad}(\nu_\mathfrak{b}\gamma_\mathfrak{b})(\delta_{\mathfrak{a}\mathfrak{b}} - \xi_\mathfrak{a}). \end{aligned} \tag{73}$$

It is seen that π does also have the meaning of a pressure. As the Lagrange multiplier associated with the saturation constraint it is called the *saturation pressure*. This saturation pressure is an independent variable. It is observed that when only a single granular phase exists, the equilibrium constitutive equations of Goodman & Cowin [11] as well as Wang & Hutter [31] for granular materials (with $\pi = 0$) are recovered. The existence of a nonvanishing scalar $\mathcal{A}_\mathfrak{a}$ gives rise to the possibility of supporting shear stress at zero shear rate, which is an important characteristic of granular materials, blood as well as high concentration suspensions. For low concentration suspensions $\mathcal{A}_\mathfrak{a} \to 0$ and the medium becomes incapable of supporting any shear stress at zero shear rate.

Finally, it should be pointed out that the constitutive relations (69)–(73) are not in agreement with those obtained by Passman et al. [23]. Using the Coleman-Noll approach of thermodynamics, their derived constitutive relations for the thermodynamic equilibrium parts $f_\mathfrak{a}^E$ and $\boldsymbol{q}^E$ are in coincidence with the expressions (69) and (71). In their form of the entropy principle the constituent entropy fluxes are from the outset assumed $\boldsymbol{\phi}_\mathfrak{a} = \boldsymbol{q}_\mathfrak{a}/\theta$, which

is equally a disadvantage of the Coleman-Noll approach, as (70) is automatically satified according to $(18)_2$, $(21)_2$ and (71). However, the constitutive relations for $\boldsymbol{T}_{\mathfrak{a}}^{E}$ and $\boldsymbol{m}_{\mathfrak{a}}^{+E}$ in [23], viz,

$$\boldsymbol{T}_{\mathfrak{a}}^{E} = -\nu_{\mathfrak{a}} p_{\mathfrak{a}} \boldsymbol{I} - \mathcal{A}_{\mathfrak{a}} \operatorname{grad} \nu_{\mathfrak{a}} \otimes \operatorname{grad} \nu_{\mathfrak{a}}, \tag{74}$$

$$\boldsymbol{m}_{\mathfrak{a}}^{+E} = \pi \operatorname{grad} \nu_{\mathfrak{a}}, \tag{75}$$

do not agree with (72) and (73). Obviously, the constitutive relations (72), (73), based on the Müller-Liu thermodynamic approach, contain more terms than those obtained by a "standard" exploitation according to Coleman-Noll. The differences are significant.

4 Saturated solid-fluid mixture with incompressible constituents

In this section we specialize this mixture theory for a specific binary mixture. We consider isothermal flows of a two-phase saturated mixture of an incompressible granular solid and a fluid. Phase f represents the fluid phase, while phase s represents the granular solid phase.

We assume that the constituent stresses $\boldsymbol{T}_{\mathfrak{a}}$, the intrinsic equilibrated body forces $f_{\mathfrak{a}}$ as well as the momentum exchange rate densities $\boldsymbol{m}_{\mathfrak{a}}^{+}$ may be decomposed according to

$$\boldsymbol{T}_{\mathfrak{a}} = \boldsymbol{T}_{\mathfrak{a}}^{E} + \boldsymbol{T}_{\mathfrak{a}}^{D},\ f_{\mathfrak{a}} = f_{\mathfrak{a}}^{E} + f_{\mathfrak{a}}^{D},\ \boldsymbol{m}_{\mathfrak{a}}^{+} = \boldsymbol{m}_{\mathfrak{a}}^{+E} + \boldsymbol{m}_{\mathfrak{a}}^{+D}, \tag{76}$$

so that

$$\begin{aligned}\theta\Pi = &-\sum \gamma_{\mathfrak{a}}\nu_{\mathfrak{a}} f_{\mathfrak{a}}^{D} \acute{\nu}_{\mathfrak{a}} + \sum \boldsymbol{T}_{\mathfrak{a}}^{D} \cdot \boldsymbol{D}_{\mathfrak{a}} - \sum \boldsymbol{m}_{\mathfrak{a}}^{+D} \cdot \boldsymbol{v}_{\mathfrak{a}} \\ &+ \left[\boldsymbol{\phi} + \frac{\partial \boldsymbol{j}_c}{\partial \theta}\right] \cdot \operatorname{grad} \theta \geq 0,\end{aligned} \tag{77}$$

where $\boldsymbol{T}_{\mathfrak{a}}^{E}$, $f_{\mathfrak{a}}^{E}$ and $\boldsymbol{m}_{\mathfrak{a}}^{+E}$ represent the thermodynamic equilibrium parts, as displayed in (69), (72) and (73), while $\boldsymbol{T}_{\mathfrak{a}}^{D}$, $f_{\mathfrak{a}}^{D}$ and $\boldsymbol{m}_{\mathfrak{a}}^{+D}$ are their dynamic contributions, which must vanish in the thermodynamic equilibrium. Relation (77) is the true dissipation inequality, and it does not involve the constraint pressure. This is proof that the constraint pressure does not produce entropy for whatever the thermodynamic pressure may be. For the dynamic parts in (76), a very useful assumption of simplification is quasi-linearity, i.e., scalar-, vector- and tensor-valued quantities are assumed to depend explicitly and linearly on scalar-vector- and tensor-valued independent dynamic variables, respectively, via scalar coefficients which themselves depend on these and on the scalar-valued independent variables. A special case of this is linearity, which arises when the scalar-valued coefficients in the quasi-linear form are assumed to depend at most on the scalar-valued independent variables. Such a form is indeed the simplest, and when there are no observations, experiments or other physical reasons to believe that the constitutive processes involved are more complicated, it seems sensible to work with this linear form. Having no such information to the contrary, and for simplicity, we assume in this work that the dynamic parts of the constituent stresses $\boldsymbol{T}_{\mathfrak{a}}$, the intrinsic equilibrated body force $f_{\mathfrak{a}}$ as well as the momentum exchange rate density $\boldsymbol{m}_{\mathfrak{a}}^{+}$ can be adequately represented by their linear forms.

$$\begin{aligned}\boldsymbol{T}_{\mathfrak{a}}^{D} &= 2\mu_{\mathfrak{a}} \boldsymbol{D}_{\mathfrak{a}}, \\ f_{\mathfrak{a}}^{D} &= \lambda_{\mathfrak{a}} \acute{\nu}_{\mathfrak{a}}, \\ \boldsymbol{m}_{\mathfrak{a}}^{+D} &= -m_D(\boldsymbol{v}_{\mathfrak{a}} - \boldsymbol{v}_{\mathfrak{b}}),\ \ (a \neq b),\end{aligned} \tag{78}$$

where $\mu_{\mathfrak{a}}$, $\lambda_{\mathfrak{a}}$, m_D are functions of $\nu_{\mathfrak{a}}$, $\operatorname{grad} \nu_{\mathfrak{a}} \cdot \operatorname{grad} \nu_{\mathfrak{a}}$, $I_{\boldsymbol{D}_{\mathfrak{a}}}$, $II_{\boldsymbol{D}_{\mathfrak{a}}}$, $III_{\boldsymbol{D}_{\mathfrak{a}}}$. Substituting (78) into the reduced entropy inequality (77) and exploiting $(67)_2$ yields the thermodynamic stability properties

$$\nu_{\mathfrak{a}}^{E} \geq 0,\ \lambda_{\mathfrak{a}}^{E} \geq 0,\ m_D^{E} \geq 0, \quad \forall \mathfrak{a}, \tag{79}$$

where the index E signifies evaluation at equilibrium.

Substituting the expressions (69), (72), (73) and (78) into (76), and the emerging expressions into equations (10), (11) and (13) yields the equations of conservation of mass, linear momentum and equilibrated forces for two incompressible constituents

$$\frac{\partial \nu_s}{\partial t} + \operatorname{div}(\nu_s \boldsymbol{v}_s) = 0, \tag{80}$$

$$\frac{\partial \nu_f}{\partial t} + \operatorname{div}(\nu_f \boldsymbol{v}_f) = 0, \tag{81}$$

$$\nu_s + \nu_f = 1, \tag{82}$$

$$\begin{aligned}&\nu_s\gamma_s\left(\frac{\partial \boldsymbol{v}_s}{\partial t} + \boldsymbol{v}_s \cdot \operatorname{grad} \boldsymbol{v}_s\right) \\ &\quad = -\operatorname{grad}\left[\nu_s(p_s + \gamma_s(\psi_I - \psi_s))\right] \\ &\qquad - \operatorname{div}\left[\mathcal{A}_s \operatorname{grad} \nu_s \otimes \operatorname{grad} \nu_s\right] \\ &\qquad + \operatorname{div}\left[\nu_s(\operatorname{grad} \boldsymbol{v}_s + (\operatorname{grad} \boldsymbol{v}_s)^T)\right] + \nu_s\gamma_s \boldsymbol{b}_s \\ &\qquad + \left[\pi + (1-\xi_s)\gamma_s(\psi_I - \psi_s) + \xi_s\gamma_f(\psi_I - \psi_f)\right] \operatorname{grad} \nu_s \\ &\qquad - m_D(\boldsymbol{v}_s - \boldsymbol{v}_f),\end{aligned} \tag{83}$$

$$\begin{aligned}&\nu_f\gamma_f\left(\frac{\partial \boldsymbol{v}_f}{\partial t} + \boldsymbol{v}_f \cdot \operatorname{grad} \boldsymbol{v}_f\right) \\ &\quad = -\operatorname{grad}\left[\nu_f(p_f + \gamma_f(\psi_I - \psi_f))\right] \\ &\qquad - \operatorname{div}\left[\mathcal{A}_f \operatorname{grad} \nu_f \otimes \operatorname{grad} \nu_f\right] \\ &\qquad + \operatorname{div}\left[\nu_f(\operatorname{grad} \boldsymbol{v}_f + (\operatorname{grad} \boldsymbol{v}_f)^T)\right] + \nu_f\gamma_f \boldsymbol{b}_f \\ &\qquad + \left[\pi + (1-\xi_s)\gamma_s(\psi_I - \psi_s) + \xi_s\gamma_f(\psi_I - \psi_f)\right] \operatorname{grad} \nu_f \\ &\qquad - m_D(\boldsymbol{v}_f - \boldsymbol{v}_s),\end{aligned} \tag{84}$$

$$\nu_s\gamma_s k_s \ddot{\nu}_s = \operatorname{div}(\mathcal{A}_s \operatorname{grad} \nu_s) + (p_s - \beta_s - \pi) + \nu_s\gamma_s\lambda_s \acute{\nu}_s, \tag{85}$$

$$\nu_f\gamma_f k_f \ddot{\nu}_f = \operatorname{div}(\mathcal{A}_f \operatorname{grad} \nu_f) + (p_f - \beta_f - \pi) + \nu_f\gamma_f\lambda_f \acute{\nu}_f. \tag{86}$$

From (85) and (86) we have

$$\begin{aligned}&\pi = p_\alpha - \beta_{\mathfrak{a}} + \operatorname{div}(\mathcal{A}_{\mathfrak{a}} \operatorname{grad} \nu_{\mathfrak{a}}) - \nu_{\mathfrak{a}}\gamma_{\mathfrak{a}} k_{\mathfrak{a}} \ddot{\nu}_{\mathfrak{a}} - \nu_{\mathfrak{a}}\gamma_{\mathfrak{a}}\lambda_{\mathfrak{a}} \acute{\nu}_{\mathfrak{a}}, \\ &\mathfrak{a} = \{s, f\},\end{aligned} \tag{87}$$

$$\beta_s - \beta_f = p_s - p_f + \operatorname{div}\left[(\mathcal{A}_s + \mathcal{A}_f)\operatorname{grad}\nu_s\right] + \nu_f\gamma_f k_f \ddot{\nu}_f - \nu_s\gamma_s k_s \ddot{\nu}_s + \nu_f\gamma_f\lambda_f\dot{\nu}_f - \nu_s\gamma_s\lambda_s\dot{\nu}_s. \tag{88}$$

Furthermore, we choose

$$\mu_s = \frac{\bar{\mu}_s \nu_s^2}{(\nu_m - \nu_s)^2} \tag{89}$$

according to Passman et al. [24] with $\bar{\mu}_s$ a constant, in which ν_m is the volume fraction corresponding to densest possible packing of the solid particles. For uniform spheres $\nu_m \approx 0.74$. Savage [25] uses essentially the same function, except with an eighth power dependence on $(\nu_m - \nu_s)$. We will assess the effects of changing this power for the later example of simple shearing flow. For the viscosity of the fluid, we let (see Passman et al. [24])

$$\mu_f = \nu_f^2 \bar{\mu}_f, \tag{90}$$

with $\bar{\mu}_f$ a constant. We also assume the drag coefficient m_D

$$m_D = \nu_s(1 - \nu_s)D, \tag{91}$$

which assures that the drag force between the constituents vanishes automatically for the limit cases $\nu_s \to 0$ and $\nu_s \to 1$.

To obtain the explicit expressions of $\boldsymbol{T}_\mathfrak{a}$, $\boldsymbol{m}_\mathfrak{a}^+$ and $f_\mathfrak{a}$, a representation for the specific free energy $\psi_\mathfrak{a}$ for each constituent $\mathfrak{a}$ is needed. We choose the simplest form according to Passman et al. [24]

$$\nu_\mathfrak{a}\gamma_\mathfrak{a}\psi_\mathfrak{a} = \phi_\mathfrak{a}(\nu_\mathfrak{a}) + \alpha_\mathfrak{a}(\operatorname{grad}\nu_\mathfrak{a} \cdot \operatorname{grad}\nu_\mathfrak{a}) \tag{92}$$

with the expressions

$$\begin{aligned} &\phi_s = a_s[\nu_s - \nu_c]^2, && a_s > 0 \\ &\phi_f = a_f[\nu_f - (1 - \nu_c)]^2, && a_f > 0, \end{aligned} \tag{93}$$

where ν_c is called the *critical volume fraction for solid particles*, above which shearing of the material will cause dilatancy, below which it will cause contraction. For uniform spheres this corresponds to a simple cubic lattice, so $\nu_c \approx 0.52$. Similarly to (89) we take

$$\alpha_s = \frac{\bar{\alpha}_s}{(\nu_m - \nu_s)^2} \tag{94}$$

for the solid constituent with $\bar{\alpha}_s$ a constant. We assume that α_f is a constant.

Substitution of the expression for the free energy (92) and the expressions for the viscosities of fluid and solid constituents (89), (90) into the field equations (80)–(86) gives eleven scalar equations for eleven unknowns ν_s, ν_f, p_s, p_f, π, the three components of $\boldsymbol{v}_s$ and the three components of $\boldsymbol{v}_f$. In the following sections we will numerically solve the differential equation system subject to appropriate boundary conditions for a typical shearing flow problem.

5 Horizontal shearing flow problem

5.1 Basis equations and boundary conditions for horizontal shearing flow

First we discuss a simple shearing problem. The boundaries are two parallel, infinite plates, a fixed distance l apart. Deformation is caused by moving one plate parallel to the other. Choose fixed Cartesian coordinates with the origin on the fixed plate, x parallel to the direction of motion of the top plate, and y orthogonal to the plates, and pointing from the fixed plate toward the moving plate against the gravity field, as shown in Fig. 1.

We consider only steady motions and assume

$$\begin{aligned} &\boldsymbol{v}_s = [v_s(y), 0, 0], \quad \boldsymbol{v}_f = [v_f(y), 0, 0], \\ &\nu_s = \nu_s(y), \ \nu_f = \nu_f(y), \ \boldsymbol{b}_s = \boldsymbol{b}_f = [0, -g, 0], \\ &p_s = p_s(y), \ p_f = p_f(y), \ \pi = \pi(y). \end{aligned} \tag{95}$$

In view of the field equations (80)–(84), (87), (88), the assumptions (95) and the expressions (89)–(94), the governing differential equations for this special problem reduce to

$$\nu_s + \nu_f = 1, \tag{96}$$

$$\frac{d}{dy}\left[\nu_s(p_s + \gamma_s(\psi_I - \psi_s)) + \mathcal{A}_s\left(\frac{d\nu_s}{dy}\right)^2\right] - \left[\pi + (1 - \xi_s)\gamma_s(\psi_I - \psi_s) + \xi_s\gamma_f(\psi_I - \psi_f)\right]\frac{d\nu_s}{dy} + g\nu_s\gamma_s = 0, \tag{97}$$

$$\frac{d}{dy}\left[\nu_f(p_f + \gamma_f(\psi_I - \psi_f)) + \mathcal{A}_f\left(\frac{d\nu_f}{dy}\right)^2\right] - \left[\pi + (1 - \xi_s)\gamma_s(\psi_I - \psi_s) + \xi_s\gamma_f(\psi_I - \psi_f)\right]\frac{d\nu_f}{dy} + g\nu_f\gamma_f = 0, \tag{98}$$

$$\frac{d}{dy}\left(\mu_s\frac{dv_s}{dy}\right) - D\nu_s(1 - \nu_s)(v_s - v_f) = 0, \tag{99}$$

$$\frac{d}{dy}\left(\mu_f\frac{dv_f}{dy}\right) - D\nu_s(1 - \nu_s)(v_f - v_s) = 0, \tag{100}$$

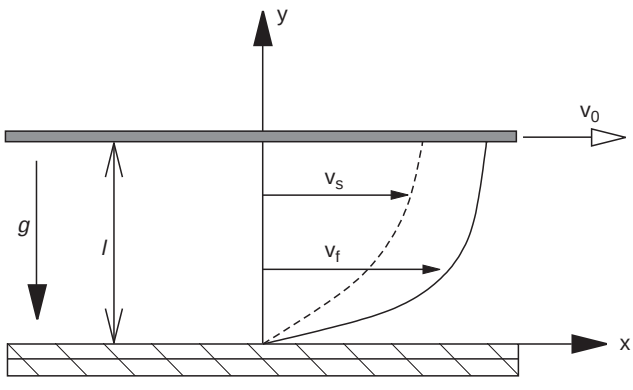

Fig. 1. Horizontal shearing flow and coordinate system

$$\pi = p_f - \beta_f + \frac{d}{dy}\left(\mathcal{A}_f \frac{d\nu_f}{dy}\right), \tag{101}$$

$$\beta_s - \beta_f = p_s - p_f + \frac{d}{dy}\left((\mathcal{A}_s + \mathcal{A}_f)\frac{d\nu_s}{dy}\right). \tag{102}$$

with

$$\nu_s\beta_s = a_s\left[\nu_s^2 - \nu_c^2\right] + \bar{\alpha}_s \frac{3\nu_s - \nu_m}{(\nu_m - \nu_s)^3}\,\mathrm{grad}\,\nu_s \cdot \mathrm{grad}\,\nu_s, \tag{103}$$

$$\nu_f\beta_f = a_f\left[\nu_f^2 - (1-\nu_c)^2\right] - \alpha_f\,\mathrm{grad}\,\nu_f \cdot \mathrm{grad}\,\nu_f, \tag{104}$$

$$\mathcal{A}_s = 2\alpha_s, \quad \mathcal{A}_f = 2\alpha_f. \tag{105}$$

Equations (96)–(102) are a system of seven equations in the seven unknowns ν_s, ν_f, π, p_s, p_f, v_s, v_f, which is second order in ν_s, ν_f, v_s and ν_f, and first order in p_s and p_f. Thus, we expect that specification of ten boundary conditions will allow us to determine ν_s, ν_f, π, p_s, p_f, v_s, v_f. We specify

$$\nu_s(0),\ \nu_s(l),\ \nu_f(0)(=1-\nu_s(0)),\ \nu_f(l)(=1-\nu_s(l)), \tag{106}$$

consistent with (102) and choose no-slip boundary conditions

$$\begin{aligned} &v_s(0) = 0,\ v_s(l) = 1,\\ &v_f(0) = 0,\ v_f(l) = 1. \end{aligned} \tag{107}$$

Here, since Eqs. (99) and (100) are linear, v_s and v_f may be nondimensionalized by dividing by the speed of the boundary $y = l$, so there is no loss of generality in choosing unity for the velocity boundary conditions at $y = l$.

For simplicity we suppose that in the upper surface the normal stress is given by

$$T_{syy}(l) = T_{fyy}(l) = -\sigma_0 \quad (\sigma_0 > 0). \tag{108}$$

We know from previous studies [22, 31] that in problems of this type, specifying the normal stress on the boundary is equivalent to specifying the flow rate.

This problem lays bare a known weakness of this theory, namely the necessity of prescribing the values of the volume fraction of the solid (and the fluid) at the plate boundaries. These are physically not controllable and thus make the solution of this problem rather academic. Another difficulty are the no-slip conditions (107) imposed upon the solid and the fluid. There could be a slip that might be tolerable. These difficulties call for a different parameterization of the stresses, not in terms of the volume fraction gradient, but rather on a rate independent stretching measure. As long as parameter studies on the influence of these boundary conditions are performed one may proceed ahead and infer consequences they imply.

5.2 Numerical method

The differential equations (96)–(102) are nonlinear. Here we solve the system of nonlinear algebra-differential equations with the boundary conditions (106)–(108) by means of the method of successive approximation. For this boundary-value problem we describe this method as follows:

We may represent equations (96)–(102) and the expressions (103)–(105) in the form (the numbers on the left indicate which eq. is involved)

$$(96)\quad \nu_f = 1 - \nu_s, \tag{109}$$

$$(103)\quad \beta_s = a_s\frac{\nu_s^2 - \nu_c^2}{\nu_s} + \bar{\alpha}_s\frac{3\nu_s - \nu_m}{\nu_s(\nu_m - \nu_s)^3}\left(\frac{\partial\nu_s}{\partial y}\right)^2, \tag{110}$$

$$(104)\quad \beta_f = a_f\frac{\nu_f^2 - (1-\nu_c)^2}{\nu_f} - \frac{\alpha_f}{\nu_f}\left(\frac{\partial\nu_f}{\partial y}\right)^2, \tag{111}$$

$$(97)\quad p_s = \frac{1}{\nu_s}\sigma_s - \gamma_s(\psi_I - \psi_s) - 2\frac{\alpha_s}{\nu_s}\left(\frac{\partial\nu_s}{\partial y}\right)^2, \tag{112}$$

$$(98)\quad p_f = \frac{1}{\nu_f}\sigma_f - \gamma_f(\psi_I - \psi_f) - 2\frac{\alpha_f}{\nu_f}\left(\frac{\partial\nu_f}{\partial y}\right)^2, \tag{113}$$

$$(101)\quad \pi = p_f - \beta_f + \frac{d}{dy}\left(2\alpha_f\frac{d\nu_f}{dy}\right), \tag{114}$$

$$(97)\quad \sigma_s = \sigma_0 + \int_y^l \Bigg\{ -[\pi + (1-\xi_s)\gamma_s(\psi_I - \psi_s) + \xi_s\gamma_f(\psi_I - \psi_f)]\frac{d\nu_s}{dy} + g\nu_s\gamma_s \Bigg\} dy, \tag{115}$$

$$(98)\quad \sigma_f = \sigma_0 + \int_y^l \Bigg\{ -[\pi + (1-\xi_s)\gamma_s(\psi_I - \psi_s) + \xi_s\gamma_f(\psi_I - \psi_f)]\frac{d\nu_f}{dy} + g\nu_f\gamma_f \Bigg\} dy, \tag{116}$$

$$(102)\quad \frac{d}{dy}\left[2(\alpha_s + \alpha_f)\frac{d\nu_s}{dy}\right] = \beta_s - \beta_f - (p_s - p_f), \tag{117}$$

$$(99)\quad \frac{d}{dy}\left(\mu_s\frac{dv_s}{dy}\right) - D\nu_s(1-\nu_s)v_s = -D\nu_s(1-\nu_s)v_f, \tag{118}$$

$$(100)\quad \frac{d}{dy}\left(\mu_f\frac{dv_f}{dy}\right) - D\nu_s(1-\nu_s)v_f = -D\nu_s(1-\nu_s)v_s, \tag{119}$$

where $\sigma_s = -T_{syy}$, $\sigma_f = -T_{fyy}$ are the normal stresses in the vertical direction. We can now define an iterative procedure which determines a sequence of functions $(\nu_s^0(y), v_s^0(y), v_f^0(y), \ldots)$, $(\nu_s^1(y), v_s^1(y), v_f^1(y), \ldots)$, $(\nu_s^2(y), v_s^2(y), v_f^2(y), \ldots)$, $\ldots$ in the following manner: $(\nu_s^0(y), v_s^0(y), v_f^0(y), \ldots)$ are chosen arbitrarily, then $(\nu_s^1(y), v_s^1(y), v_f^1(y), \ldots)$, $(\nu_s^2(y), v_s^2(y), v_f^2(y), \ldots), \ldots$ are calculated successively as the solutions of the boundary-value problem

$$\frac{d}{dy}\left[2(\alpha_s^k + \alpha_f)\frac{d\tilde{\nu}_s^{k+1}}{dy}\right] = \beta_s^k - \beta_f^k - (p_s^k - p_f^k), \tag{120}$$

$$\frac{d}{dy}\left(\mu_s^k\frac{d\tilde{v}_s^{k+1}}{dy}\right) - D\nu_s^k(1-\nu_s^k)\tilde{v}_s^{k+1} = -D\nu_s^k(1-\nu_s^k)v_f^k, \tag{121}$$

$$\frac{d}{dy}\left(\mu_f^k \frac{d\tilde{v}_f^{k+1}}{dy}\right) - D\nu_s^k(1-\nu_s^k)\tilde{v}_f^{k+1} = -D\nu_s^k(1-\nu_s^k)v_s^k \tag{122}$$

subject to the boundary conditions (106), (107), with the expressions

$$\nu_f^k = 1 - \nu_s^k, \tag{123}$$

$$\beta_s^k = a_s \frac{\nu_s^{k2} - \nu_c^2}{\nu_s^k} + \bar{\alpha}_s \frac{3\nu_s^k - \nu_m}{\nu_s^k(\nu_m - \nu_s^k)^3}\left(\frac{\partial \nu_s^k}{\partial y}\right)^2, \tag{124}$$

$$\beta_f^k = a_f \frac{\nu_f^{k2} - (1-\nu_c)^2}{\nu_f^k} - \frac{\alpha_f}{\nu_f^k}\left(\frac{\partial \nu_f^k}{\partial y}\right)^2, \tag{125}$$

$$p_s^k = \frac{1}{\nu_s^k}\sigma_s^k - \gamma_s(\psi_I^k - \psi_s^k) - 2\frac{\bar{\alpha}_s}{\nu_s^k(\nu_m - \nu_s^k)^2}\left(\frac{\partial \nu_s^k}{\partial y}\right)^2, \tag{126}$$

$$p_f^k = \frac{1}{\nu_f^k}\sigma_f^k - \gamma_f(\psi_I^k - \psi_f^k) - 2\frac{\alpha_f}{\nu_f^k}\left(\frac{\partial \nu_f^k}{\partial y}\right)^2, \tag{127}$$

$$\pi^k = p_f^k - \beta_f^k + \frac{d}{dy}\left(2\alpha_f \frac{d\nu_f^k}{dy}\right), \tag{128}$$

$$\sigma_s^{k+1} = \sigma_0 + \int_y^l \Big\{ -[\pi^k + (1-\xi_s^k)\gamma_s(\psi_I^k - \psi_s^k) + \xi_s^k\gamma_f(\psi_I^k - \psi_f^k)]\frac{d\nu_s^k}{dy} + g\nu_s^k\gamma_s \Big\} dy, \tag{129}$$

$$\sigma_f^{k+1} = \sigma_0 + \int_y^l \Big\{ -[\pi^k + (1-\xi_s^k)\gamma_s(\psi_I^k - \psi_s^k) + \xi_s^k\gamma_f(\psi_I^k - \psi_f^k)]\frac{d\nu_f^k}{dy} + g\nu_f^k\gamma_f \Big\} dy. \tag{130}$$

We can discretize the equations (120)–(122) for n uniform distributed discrete points in $y \in [0, l]$ by finite-difference approximations with central finite-difference quotients. In so doing, for each iterative step three tri-diagonal systems emerge, for $\tilde{\nu}_s^{k+1}$ from equation (120), for $\tilde{v}_s^{k+1}$ from (121) and for $\tilde{v}_f^{k+1}$ from (122), respectively. We can solve this boundary-value problem e.g. by Gaussian elimination to obtain $\tilde{\nu}_s^{k+1}$, $\tilde{v}_s^{k+1}$ and $\tilde{v}_f^{k+1}$, then ν_s^{k+1}, v_s^{k+1} and v_f^{k+1} are defined by the over-relaxation iteration by the formulas

$$\left.\begin{aligned} \nu_s^{k+1} &= \nu_s^k + \tau(\tilde{\nu}_s^{k+1} - \nu_s^k), \\ v_s^{k+1} &= v_s^k + \tau(\tilde{v}_s^{k+1} - v_s^k), \\ v_f^{k+1} &= v_f^k + \tau(\tilde{v}_f^{k+1} - v_f^k), \end{aligned}\right\} \quad 0 < \tau \le 1, \tag{131}$$

where τ is a positive real parameter. We should choose τ so small that convergent iteration is reached. We would like to point out that this iterative choice is not the only possible one.

We start with the initial trial functions

$$\nu_s^0 = \nu_s(0) + \frac{y}{l}(\nu_s(l) - \nu_s(0)), \quad v_s^0 = \frac{y}{l}, \quad v_f^0 = \frac{y}{l}, \tag{132}$$

which statisfy the boundary conditions. The iteration should be carried out until the relative differences of the computed ν_s, v_s and v_f between two iterative steps are smaller than a given error, respectively, chosen to be 10^{-6}.

5.3 Numerical results

We choose to investigate the case with estimated parameters corresponding to a mixture of water with natural angular beach sand (average particle diameter 0.04 cm). For this mixture, the values for $\gamma_{\mathfrak{a}}$, $\mu_{\mathfrak{a}}$ and ν_m are given according to Passman et al. [24] by

$$\begin{aligned} &\gamma_s = 2200\,\mathrm{kg\,m^{-3}},\ \bar{\mu}_s = 723\,\mathrm{kg\,m^{-1}\,s^{-1}}, \\ &\nu_m = 0.74,\ \gamma_f = 1000\,\mathrm{kg\,m^{-3}}, \\ &\bar{\mu}_f = 0.001\,\mathrm{kg\,m^{-1}\,s^{-1}}. \end{aligned} \tag{133}$$

The values of parameters $\alpha_{\mathfrak{a}}$, $a_{\mathfrak{a}}$ are somewhat problematic. We take as values

$$\begin{aligned} &\bar{\alpha}_s = 4.0 \times 10^{-5}\,\mathrm{kg\,m\,s^{-2}}, \\ &\alpha_f = 3.0 \times 10^{-5}\,\mathrm{kg\,m\,s^{-2}}, \\ &a_s = 20\,\mathrm{kg\,m^{-1}\,s^{-2}\,(Pa)}, \\ &a_f = 10\,\mathrm{kg\,m^{-1}\,s^{-2}\,(Pa)}, \end{aligned} \tag{134}$$

for initial computational investigation and later assess the effects of changing them. For the drag coefficient D we choose

$$D \in [0, 10^5]\,\mathrm{kg\,m^{-3}\,s^{-1}} \tag{135}$$

to perform our computations. It is even more problematic as to what boundary conditions to assign to $\nu_s(0)$, $\nu_s(l)$. We know of no evidence, experimental or otherwise, which would guide the choice of either of these two numbers for types of physical boundaries we assume, and indeed, although our numerical scheme works successfully for any $\nu_s(0) \in (0, \nu_m]$, $\nu_s(l) \in (0, \nu_m]$, our choices are essentially arbitrary. In our computations we first take

$$\nu_s(0) = 0.7,\ \nu_s(l) = 0.3 \tag{136}$$

and later assess the effect of changing them.

We have done an extensive parametric study for this problem, which is not presented in detail here. Instead, a few representative volume fraction, velocity and normal stress profiles will be included with a discussion of effects of the parameters.

The results for the parameter choices (134), (135) and the boundary conditions (107), (108) with $\sigma_0 = 0$ as well as (136) are shown in Figs. 2a–d. The solid-volume fraction (Fig. 2a) decreases initially only very slowly from its boundary value as the distance from the bottom increases. As the distance increases, this decrease becomes rapid, specially in the top region of the cross section. The normal stresses for the solid and the fluid (Fig. 2b) increase approximately linearly from their given zero boundary value at the top as the depth increases. The solid normal stress is considerably larger than that of the fluid except for

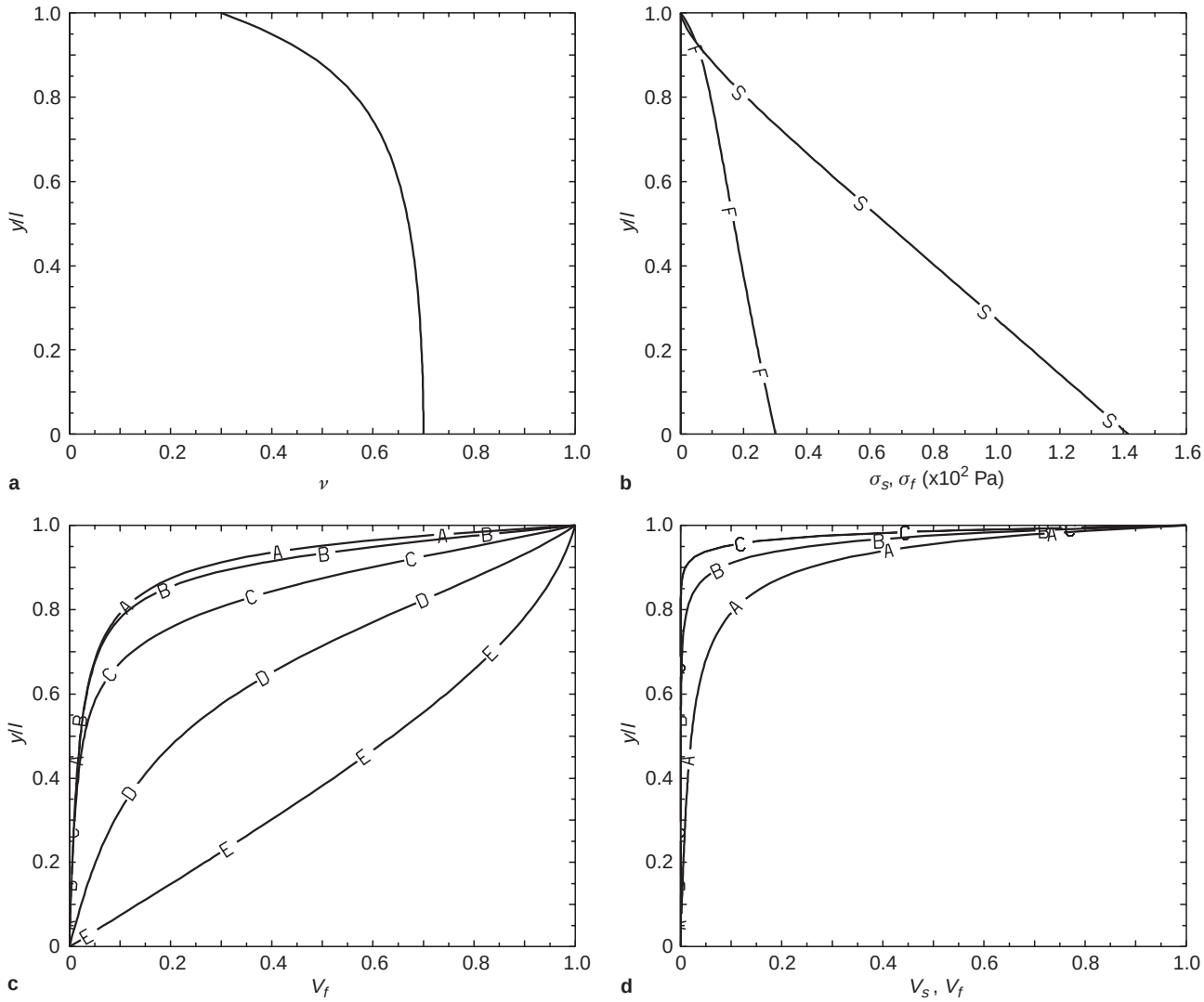

Fig. 2. **a** Solid volume fraction profile. **b** Normal solid and fluid stress profiles. S: Solid; F: Fluid. **c** Nondimensional fluid velocity profiles for various values of the drag coefficient D. $D = 10^5\,(A),\ 10^4\,(B),\ 10^3\,(C),\ 10^2\,(D),\ 0\,(E)\,\mathrm{kg\,m^{-3}\,s^{-1}}$. The solid velocity for these cases is almost the same as the fluid velocity (A). **d** Nondimensional (solid or fluid) velocity profiles for $D = 10^5\,\mathrm{kg\,m^{-3}\,s^{-1}}$ with various values of power $n = 2\,(A),\ 4\,(B),\ 8\,(C)$ (instead of $n = 2$ for **c**) in the function (89) $\mu_s = (\bar{\mu}_s \nu_s^2)/(\nu_m - \nu_s)^n$. The other parameters are: $\bar{\alpha}_s = 4.0 \times 10^{-5}\,\mathrm{kg\,m\,s^{-2}}$, $\alpha_f = 3.0 \times 10^{-5}\,\mathrm{kg\,m\,s^{-2}}$, $a_s = 20\,\mathrm{kg\,m^{-1}\,s^{-2}}$, $a_f = 10\,\mathrm{kg\,m^{-1}\,s^{-2}}$, $\nu_s(0) = 0.7$, $\nu_s(l) = 0.3$, $\sigma_0 = 0$, $l = 0.01\,\mathrm{m}$

the very small zone at the top. The fluid velocity profiles for various values of the drag coefficient D are shown in Fig. 2c. All parameters are the same as in Fig. 2a, b. For the case of $D = 10^5\,\mathrm{kg\,m^{-3}\,s^{-1}}$ the solid velocity is nearly the same as that of the fluid (for curve A in the graph), and decreasing the value of D decreases the solid velocity only very slightly so that we do not show it in the figure. The value of the fluid velocity increases considerably when the value of D is decreased, a fact that is expected as D measures the Darcy drag. For $D = 0$ the fluid constituent behaves very similar to a viscous fluid flow. On the other hand, the solid flow occurs mainly only near the top. Comparision of the solid velocity profile (curve A in Fig. 2c) with the solid volume fraction (Fig. 2a) shows that near the top the shearing of the material causes dilatancy. Qualitatively, these results are similar to those obtained by Passman et al. [24], although the used constitutive equations in the two models are significantly different. That is to say that the additional terms in the constitutive relations obtained in the evalution of the entropy principle following the concept of Müller and Liu play not a very significant role in this numerical example of simple shearing, but we still cannot say that these terms are not important for all flow problems. We need further study in what cases these additional terms may be important.

In the above computations we have empolyed an expression of the solid viscosity in the form

$$\mu_s = \frac{\bar{\mu}_s \nu_s^2}{(\nu_m - \nu_s)^n}. \tag{137}$$

with $n = 2$ according to Passman et al. [24] (see eq. (89)), which is different from Savage's choice [25] with a power $n = 8$. We have also assessed the effect of the value of the

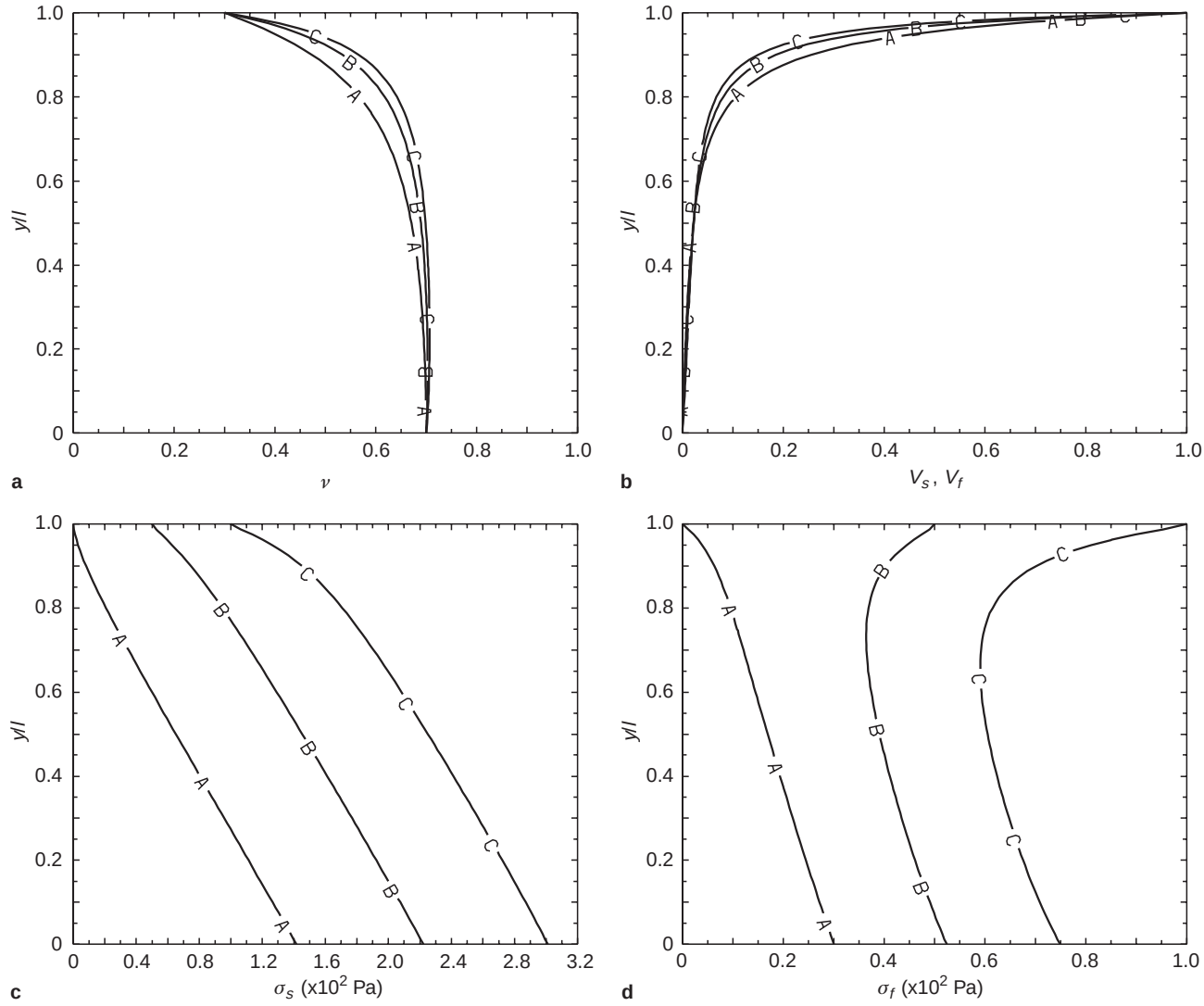

Fig. 3. **a** Solid volume fraction profiles. **b** Nondimensional velocity profiles. **c** Normal solid stress profiles. **d** Normal fluid stress profiles. Here nothing has been changed from the case shown in Figs. 2a–c for $D = 10^5\,\mathrm{kg\,m^{-3}\,s^{-1}}$, except with various values of the normal stress at the top σ_0 (instead of $\sigma_0 = 0$): A: $\sigma_0 = 0\,\mathrm{Pa}$; B: $\sigma_0 = 50\,\mathrm{Pa}$; C: $\sigma_0 = 100\,\mathrm{Pa}$

power in the expression of the solid viscosity, with $n = 2, 4, 8$ instead of $n = 2$. The results are shown in Fig. 2d for the solid and fluid velocities which are almost identical for $D = 10^5\,\mathrm{kg\,m^{-3}\,s^{-1}}$. Increasing the value of the power n tends to bound the solid flow toward a thinner layer at the top; this is not the same as obtained by Passman et al. who claimed that *the exact value of this power, as long as it is positive and even, appears to have little effect on the character of the flow.*

Computations have also been performed for various other values of the normal stress. Fig. 3 shows the effect of changing the normal top-wall stress on the horizontal mixture shearing flow, where nothing has been changed from the case shown in Figs. 2a–c, except the value of the normal top-wall stress and the drag coefficient is fixed at $D = 10^5\,\mathrm{kg\,m^{-3}\,s^{-1}}$. Increasing the normal stress will tend to cause the grains to interlock and increase ν throughout the flow field (Fig. 3a). For large values of D (here $D = 10^5\,\mathrm{kg\,m^{-3}\,s^{-1}}$) the solid and fluid velocity profiles are approximately the same (Fig. 3b). As the normal stress increases, the grain motion has an increasing tendency toward a rigid motion in the larger region near the bottom, while the shearing layer near the top becomes thinner. The normal solid and fluid stresses (Figs. 3c–d) do no longer increase approximately linearly with increasing depth as for the case with $\sigma_0 = 0$ (curve A). Specifically, for the normal fluid stress, if the normal top-stress is sufficiently large, the normal fluid stress decreases initially with increasing distance from the top and then increases. There is even a case for which the normal fluid stress at the bottom is smaller than that at the top (curve C in Fig. 3d).

Fig. 4 demonstrates the effect of varying the distance of the two plates on the volume fraction, velocity and normal stress. It can be seen from Figs. 4a, b that a wide channel shows a relative large interlock layer near the bottom with an almost constant volume fraction, while, as the channel width decreases, there is an increasing tendency to extend the shearing and dilatant layer near

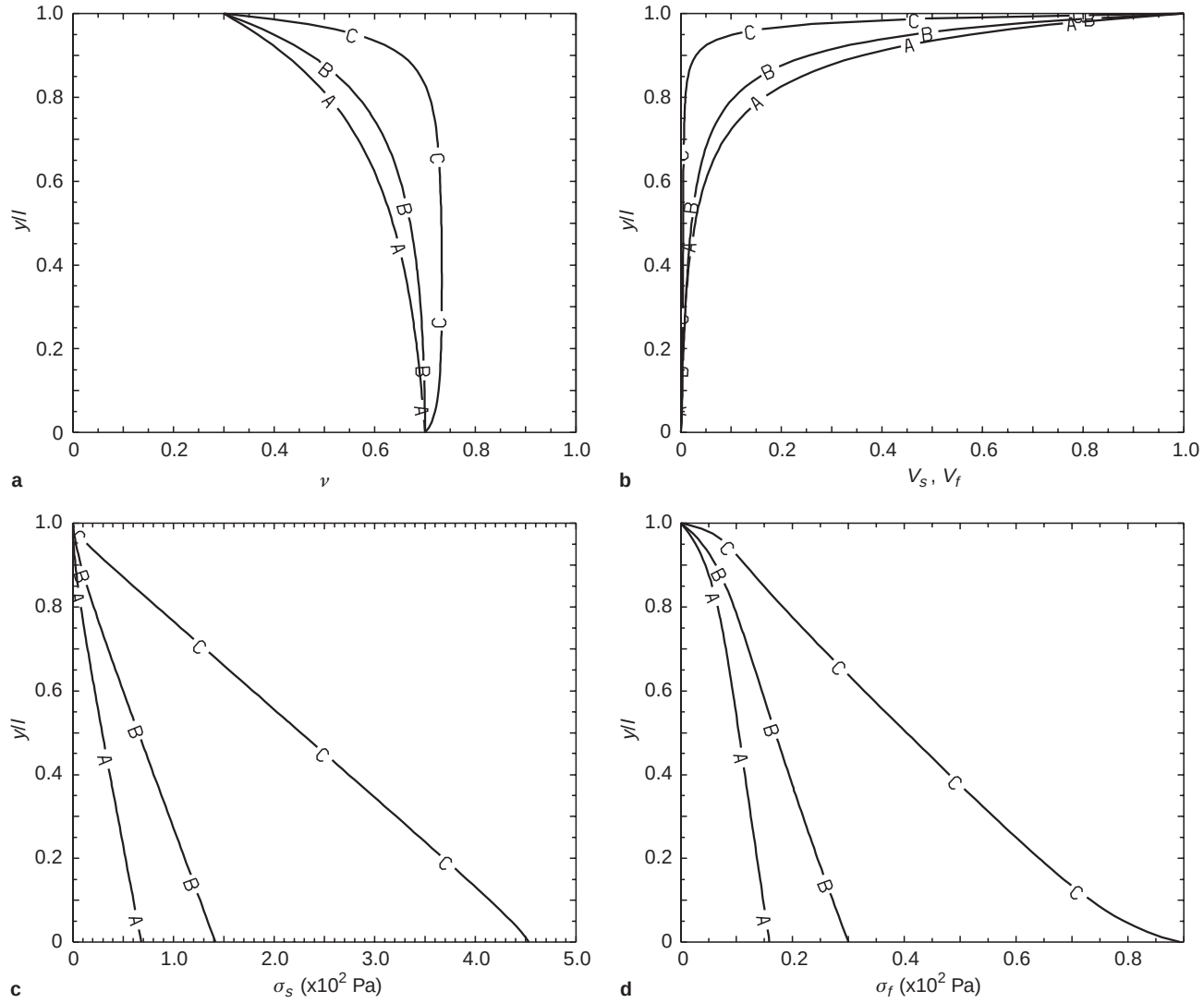

Fig. 4. **a** Solid volume fraction profiles. **b** Nondimensional velocity profiles. **c** Normal solid stress profiles. **d** Normal fluid stress profiles. All parameters are the same as in Figs. 2**a**–**c** and $D = 10^5\,\mathrm{kg\,m^{-3}\,s^{-1}}$, except the distance of the plates l. A: $l = 0.5\,\mathrm{cm}$; B: $l = 1.0\,\mathrm{cm}$; C: $l = 3.0\,\mathrm{cm}$

the top. However the absolute value of the shearing layer thickness is less influenced, which is approximately between 5 and 15 grain diameters. The normal solid and fluid stresses, shown in Figs. 4c,d, as expected increase when the channel width increases.

We have also investigated the effect of changing α_s and α_f by changing each by factors of 0.1, 10, 100, using the case in Figs. 2a–c with $D = 10^5\,\mathrm{kg\,m^{-3}\,s^{-1}}$ as a basis. These results are displayed in Fig. 5. As the values of α_s and α_f are increased, the curvatures of the volume fraction and velocity profiles are decreased, i.e., increasing α_s and α_f enlarges the shearing zone near the top and reduces the interlock zone near the bottom. The shear rate at the top is, of course, decreased accordingly. It can also be seen from Figs. 5a, b that for sufficiently large values of α_s and α_f, ($\bar{\alpha}_s > 4.0 \times 10^{-4}\,\mathrm{kg\,m\,s^{-2}}$ and $\alpha_f > 3.0 \times 10^{-4}\,\mathrm{kg\,m\,s^{-2}}$) the volume fraction and the velocity profiles are influenced only very slightly by varying $\bar{\alpha}_s$ and α_f. Interesting is that the normal solid stress decreases by increasing $\bar{\alpha}_s$ and α_f (Fig. 5c), whereas the normal fluid stress changes in the reverse way (Fig. 5d). This behaviour is also fairly different from varying of the volume fraction and the velocity; the normal stresses vary still, even more, rapidly with $\bar{\alpha}_s$ and α_f for $\bar{\alpha}_s > 4.0 \times 10^{-4}\,\mathrm{kg\,m\,s^{-2}}$ and $\alpha_f > 3.0 \times 10^{-4}\,\mathrm{kg\,m\,s^{-2}}$, which we can see from Figs. 5c, d. A possible reason is that, for small α_s and α_f, the change of the normal stresses by varying α_s and α_f is compensated by a corresponding change in volume fraction. When α_s and α_f are large enough ($\bar{\alpha}_s > 4.0 \times 10^{-4}\,\mathrm{kg\,m\,s^{-2}}$ and $\alpha_f > 3.0 \times 10^{-4}\,\mathrm{kg\,m\,s^{-2}}$), the volume fraction remains nearly unchanged when α_s and α_f are varied; in this case, the influence of varying α_s and α_f manifests itself mainly in the change of the normal stresses. Besides, there exists even a negative normal solid stress (tensile) zone near the top for large $\bar{\alpha}_s$ and α_f (curve D in Fig. 5c), which is perhaps unphysical because

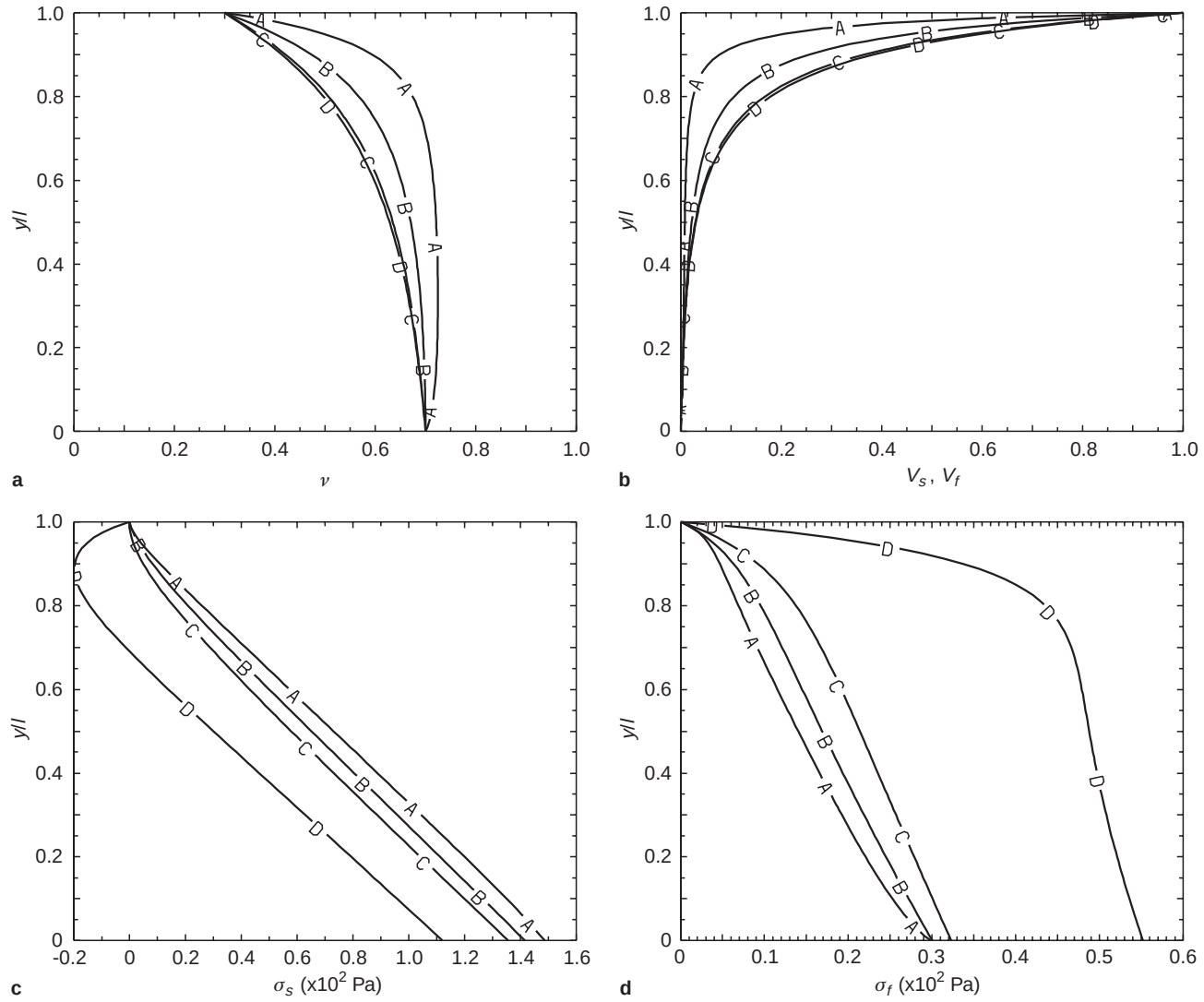

Fig. 5. **a** Solid volume fraction profiles. **b** Nondimensional velocity profiles. **c** Normal solid stress profiles. **d** Normal fluid stress profiles. Here nothing has been changed from the case shown in Figs. 2**a–c** for $D = 10^5\,\mathrm{kg\,m^{-3}\,s^{-1}}$, except the values of $\bar{\alpha}_s$, α_f. A: $(\bar{\alpha}_s, \alpha_f) = (4.0, 3.0) \times 10^{-6}\,\mathrm{kg\,m\,s^{-2}}$; B: $(\bar{\alpha}_s, \alpha_f) = (4.0, 3.0) \times 10^{-5}\,\mathrm{kg\,m\,s^{-2}}$; C: $(\bar{\alpha}_s, \alpha_f) = (4.0, 3.0) \times 10^{-4}\,\mathrm{kg\,m\,s^{-2}}$; D: $(\bar{\alpha}_s, \alpha_f) = (4.0, 3.0) \times 10^{-3}\,\mathrm{kg\,m\,s^{-2}}$

the values of α_s and α_f exceed the physically reasonable range.

We also investigated the effect of changing a_s and a_f by changing the value of each variable by factors of 0.1, 10, 100, using the case in Figs. 2a–c with $D = 10^5\,\mathrm{kg\,m^{-3}\,s^{-1}}$ as a basis. It can be seen from Figs. 6a, b that decreasing a_s and a_f has the effect of causing an even larger region near the bottom where the solid-volume fraction profile remains close to constant (the boundary value), and correspondingly causing a somewhat larger region where the motion is almost rigid, with a smaller region of even higher shear rate. These features of varying a_s and a_f are very similar to those of varying α_s and α_f. The difference from those of varying α_s and α_f is that for sufficiently small values of a_s and a_f ($a_s < 20\,\mathrm{Pa}$ and $a_f < 10\,\mathrm{Pa}$) the volume fraction and the velocity profiles vary only slightly by varying a_s and a_f, which can be seen in Figs. 6c, d. Increasing a_s and a_f decreases the normal solid stress, but increases the normal fluid stress, which is similar to varying α_s and α_f. It is of interest to note that the normal stresses at the bottom are essentially unaffected by varying a_s, a_f.

The effect of changing boundary conditions $\nu_s(0)$ and $\nu_s(l)$ is illustrated in Figs. 7, 8. Here, all parameters are exactly the same as in Figs. 2a–c, except that the solid-volume fraction at the bottom has been set equal to $\nu_s(0) = 0.72$, a value very close to ν_m, and at the top $\nu_s(l) = 0.02$, i.e., almost only fluid constituent exists (Fig. 7), as well as $\nu_s(0) = \nu_s(l) = 0.4$ (Fig. 8), respectively.

Fig. 7a indicates that, for the case that the solid-volume fraction at the bottom attains its possible maximum and at the top nearly only fluid constituent is present, the solid-volume fraction decreases only slightly from its boundary value with the distance from the bottom over approximately a half of the cross section, then

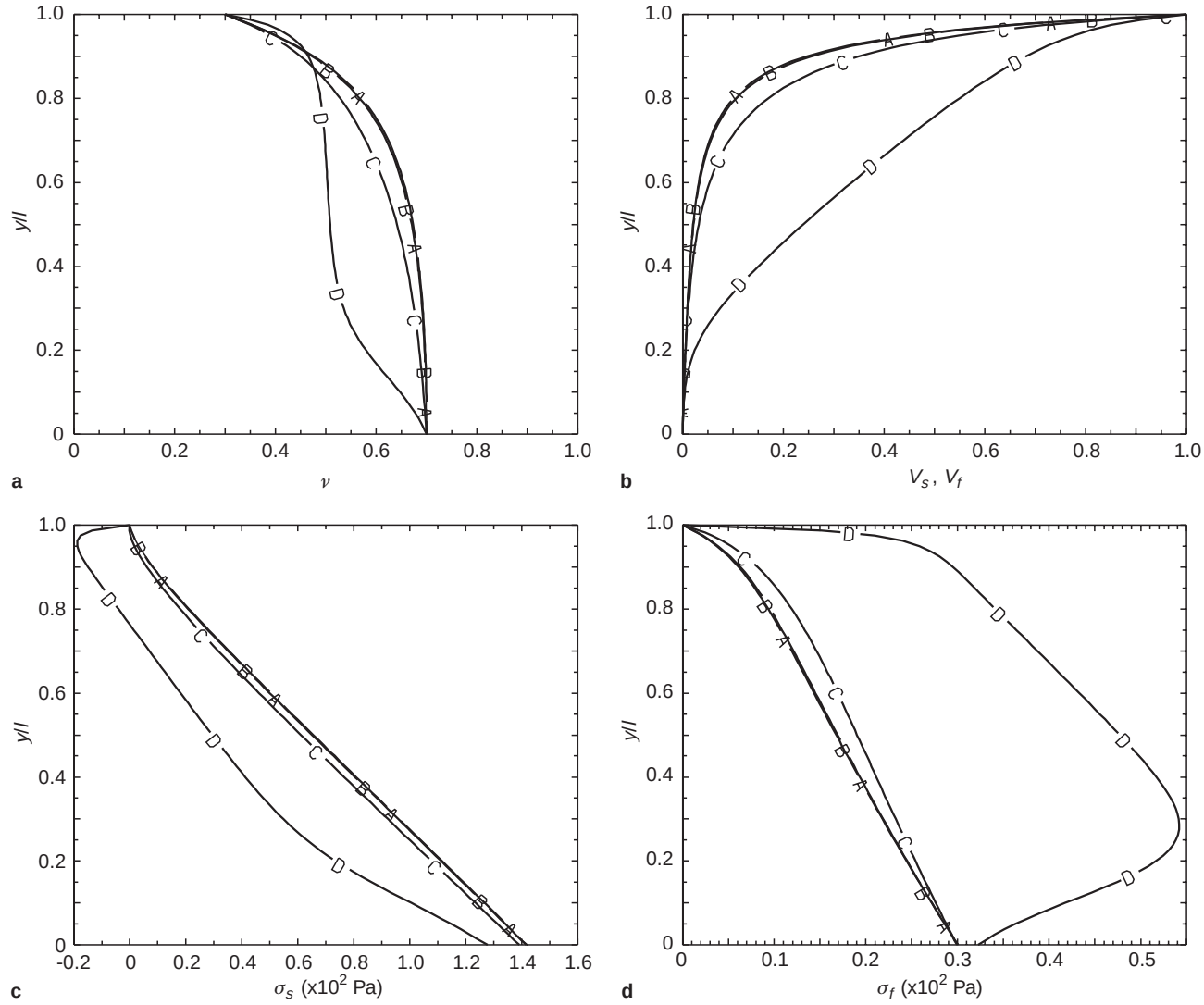

Fig. 6. **a** Solid volume fraction profiles. **b** Nondimensional velocity profiles. **c** Normal solid stress profiles. **d** Normal fluid stress profiles. Here nothing has been changed from the case shown in Figs. 2**a**–**c** for $D = 10^5\,\mathrm{kg\,m^{-3}\,s^{-1}}$, except the values of a_s, a_f. A: $(a_s, a_f) = (2, 1)\,\mathrm{Pa}$; B: $(a_s, a_f) = (20, 10)\,\mathrm{Pa}$; C: $(a_s, a_f) = (200, 100)\,\mathrm{Pa}$; D: $(a_s, a_f) = (2000, 1000)\,\mathrm{Pa}$

there is a sudden decrease and at the top one-tenths of the cross section the decrease becomes slower again. This resembles a two layer effect: a thick solid layer near the bottom and a very thin fluid layer near the top. For this case the normal fluid stress increases rapidly at the top two-tenths of the cross section with decreasing distance from the top, then varies only very slightly, while against it, the normal solid stress decreases only slightly at the top two-tenths of the cross section from its zero boundary value, then increases almost linearly with the increasing depth, as demonstrated in Fig. 7b. The corresponding solid and fluid velocity profiles are displayed in Fig. 7c for various values of drag coefficient D. Because of a fairly low solid-volume fraction near the top, the solid and fluid velocities are visibly different, even though $D = 10^5\,\mathrm{kg\,m^{-3}\,s^{-1}}$. The graph S indicates the solid velocity, which is principally independent of the value of D. A solid motion of high shear rate exists only in a very small region at the top. In the remaining large lower region the solid motion vanishes. It clearly demonstrates the existence of an internal boundary separating a shearing region from a rigid region. The fluid motion for a large value of D is very similar to that of the solid, with appreciable values only in a thin layer near the top. Decreasing D extends the region of the fluid motion till the bottom. For very small D the fluid constituent behaves nearly as a viscous fluid.

For the boundary conditions that the solid-volume fraction at the top and at the bottom possesses the same value $\nu_s(0) = \nu_s(l) = 0.4$, it can be seen from Fig. 8a that, in addition to the increase in the solid-volume fraction in the neighborhood of the top plate, which is similar to Fig. 2a, there is an increase also in the neighborhood of the bottom plate. The volume fraction diagram is,

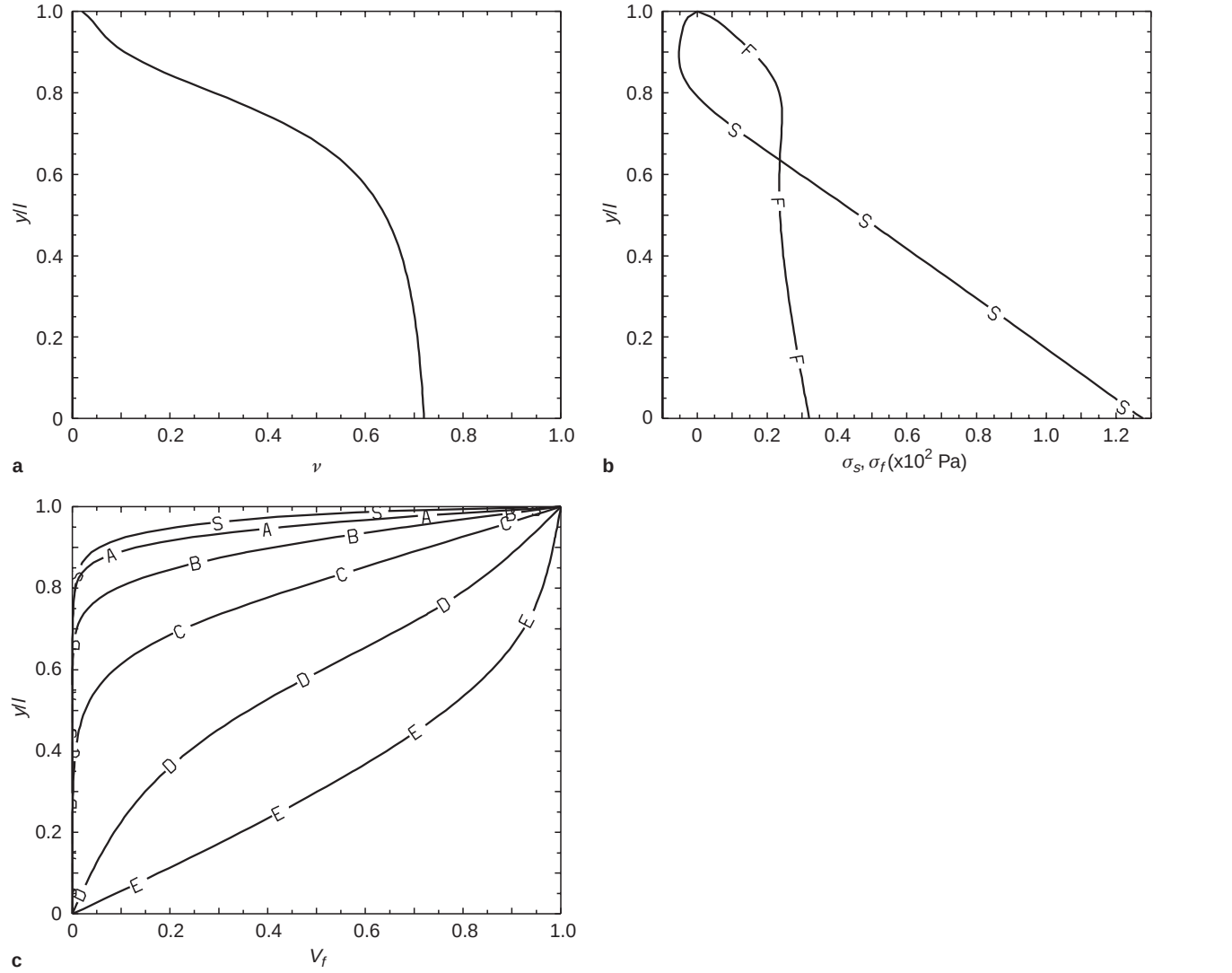

Fig. 7. a Solid volume fraction profiles. **b** Normal solid (S) and fluid (F) stress profiles. **c** Nondimensional velocity profiles. S: Solid velocity. A–E: Fluid velocity for various values of the drag coefficient D. $D = 10^5\,(A),\ 10^4\,(B),\ 10^3\,(C),\ 10^2\,(D), 0\,(E)$ $\mathrm{kg\,m^{-3}s^{-1}}$. All parameters are the same as in Figs. 2**a**–**c**, except the boundary values of the volume fraction $\nu_s(0) = 0.72,\ \nu_s(l) = 0.02$

of course, unsymmetric in the obvious way because of gravity. In both cases, the region of the low solid-volume fraction is a region of high shear rate (Fig. 8c as well as Fig. 2c), which may lead back to the effect of dilatancy in granular materials. For the high drag coefficient $D = 10^5\,\mathrm{kg\,m^{-3}\,s^{-1}}$, the velocities of the two constituents again are virtually indistinguishable. As before, the solid velocity is nearly independent of D (graph A), while the fluid velocity profiles become less astute with decreasing D, close to that of a viscous fluid. The normal stresses increase monotonously with increasing depth with the exception of the normal solid stress near the bottom.

6
Concluding remarks

In this paper a thermodynamic theory for a multiphase mixture, specially for a solid-fluid mixture was presented in which, besides balances for mass, momentum and energy, a balance law for equilibrated forces, as proposed by Goodman & Cowinfor dry granular and then used by Passman et al. for mixtures, was introduced, for each constituent of mixture, to accommodate for the dynamical effects played by the volume fraction. The form of the entropy principle of mixture imposed on a postulated constitutive relation was that of Müller-Liu, i.e., for the prescribed constitutive class the entropy inequality was identically satisfied under the constraints that the balance laws of mass, momentum, energy and equilibrated forces of all constituents (with or without supply terms), as well as a saturation condition be satisfied. It was shown that in comparison to a "standard" exploitation according to Coleman-Noll from Passman et al. [23], in which momentum, energy and equilibrated force sources of arbitray value are permitted, the constitutive relations based on the more general Müller-Liu thermodynamic

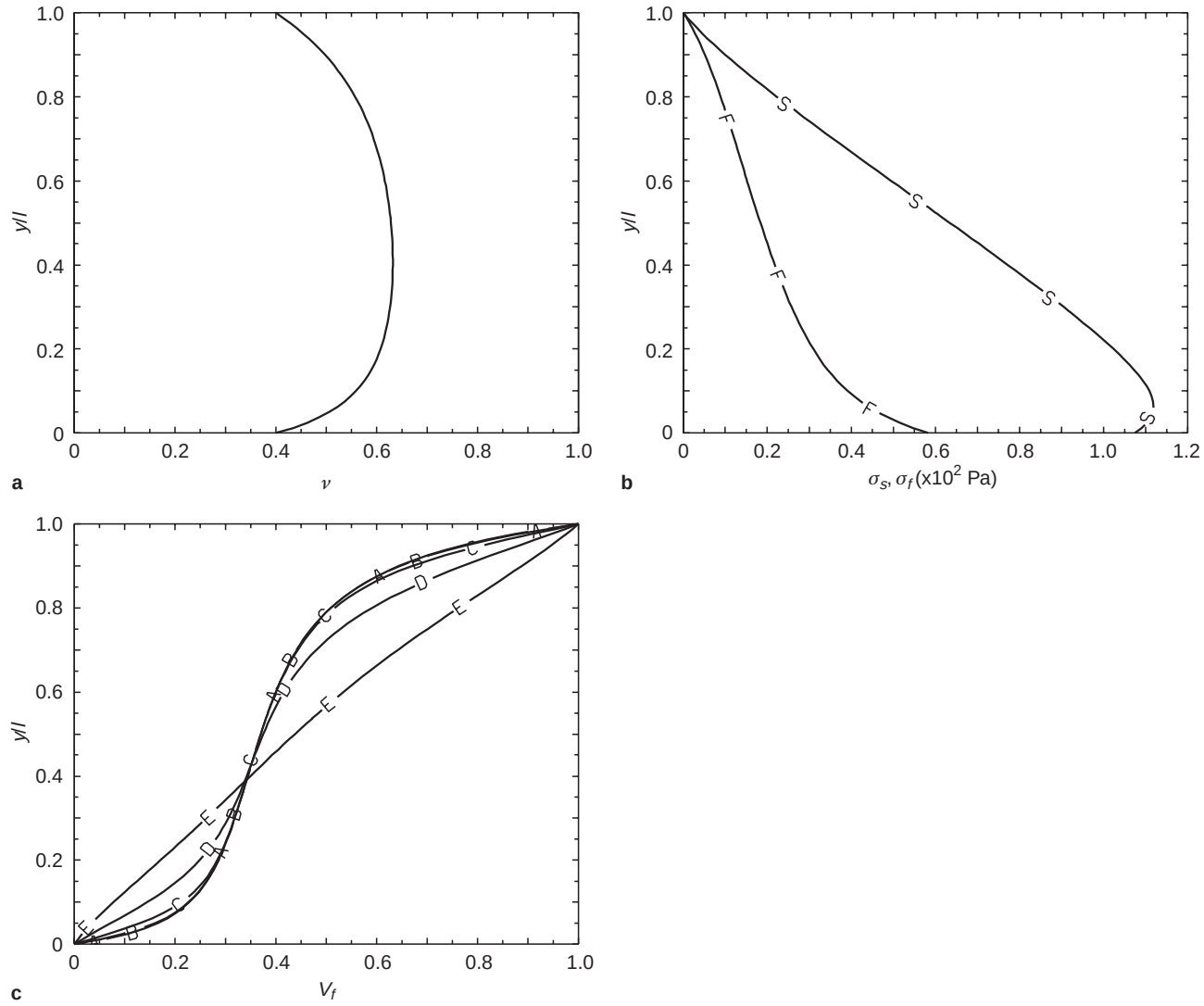

Fig. 8. **a** Solid volume fraction profiles. **b** Normal solid (S) and fluid (F) stress profiles. **c** Nondimensional velocity profiles for various values of the drag coefficient D. $D = 10^5\,(A),\ 10^4\,(B),\ 10^3\,(C),\ 10^2\,(D),\ 0\,(E)\ \ \mathrm{kg\,m^{-3}\,s^{-1}}$. The solid velocity for these cases is almost the same as the fluid velocity (A). All parameters are the same as in Figs. 2**a**–**c**, except the boundary values of the volume fraction $\nu_s(0) = 0.4,\ \nu_s(l) = 0.4$

consideration are different. This theory was applied to analyses of steady fully-developed horizontal shearing flow of a saturated solid-fluid mixture with incompressible constituents. The partly numerical results are in qualitative agreement with those obtained by Passman et al. [24], although the used constitutive equations in the two models are not quite the same. Most results showed that the flow was divided in two regimes of behaviour by the existence of an internal boundary above which the granular material deformed rapidly, but below which the granular material remained rigidly locked in place. This feature is in qualitative agreement with experimental results by Hanes and Inman [12]. Their experiments clearly demonstrate the existence of an internal boundary separating a shearing region from a rigid region. The thickness of the shearing region was measured to be between 5 and 15 grain diameters. In our computional results the thickness of the shearing layer also lays approximately in this range.

References

1. G. Ahmadi: On mechanics of saturated granular materials. Int. J. Non-linear Mechanics, **15** (1980), 251–262
2. G. Ahmadi: A continuum theory for two phase media. Acta Mech. **44** (1982), 299–317
3. R. A. Bagnold: Experiments on a gravity free dispersion of large solid spheres in a Newtonian fluid under shear. Proc. Roy. Soc. (London) **A225** (1954), 49–63
4. J. A. Bailard: An experimental study of granular fluid flow. Thesis, Uni. California, San Diego (1978)
5. J. Bluhm, R. de Boer & K. Wilmanski: The thermodynamic structure of the two component model of porous incompressible materials with true mass densities. Mech. Res. Comm., **22**(2) (1995), 171–180
6. R. M. Bowen: Incompressible porous media models by use of the theory of mixtures. Int. J. Engng Sci., **18** (1980), 1129–1148
7. R. M. Bowen: Compressible porous media models by use of the theory of mixtures. Int. J. Engng Sci., **20** (1982), 697–735

8. B. D. Coleman & W. Noll: The thermodynamics of elastic materials with heat conduction and viscosity. Arch. Rat. Mech. and Anal., **13** (1963), 245–261
9. W. Ehlers, Compressible, incompressible and hybrid two-phase models in porous media theories. In Anisotropy and Inhomogeneity in Elasticity and Plasticity, edited by Y. C. Angel (AMD-Vol. 158, ASME, New York, 1993), pp. 25–38
10. W. Ehlers & J. Kubik: On finite dynamic equations for fluid-saturated porous media. Acta Mechanica, **105** (1994), 101–117
11. M. A. Goodman & S. C. Cowin: A continuum theory for granular materials. Arch. Rat. Mech. and Anal., **44** (1972), 249–266
12. D. M. Hanes & D. L. Inman: Observations of rapidly flowing granular-fluid materials. J. Fluid Mech. **150** (1985), 357–380
13. G. Homsy, M. M. Ei-Kaissay, & A. Didwania: Instability waves and theorigin of bubbles in fluidized beds, part 2: comparison with theory. Int. J. Multiphase Flow, **6** (1980), 305–318
14. K. Hutter and K. R. Rajagopal: On flows of granular materials. Continuum Mech. Thermodyn., **6** (1994), 81–139
15. K. Hutter, B. Svendsen, & D. Rickenmann: Debris flow modeling: A review Continuum Mech. Thermodyn., **8** (1996), 1–35
16. G. Johnson, M. Massoudi, & K. R. Rajagopal: Flow of a fluid-solid mixture between flat plates. Chemical Engineering Science, **46**(7) (1991), 1713–1723
17. I-Shih Liu: Method of Lagrange multipliers for exploitation of the entropy principle. Arch. Rat. Mech. and Anal., **46** (1972), 131–148
18. I-Shih Liu & I. Müller (1984) Thermodynamics of mixtures of fluids. In: Truesdell, C. (ed): Rational thermodynamics, pp 264–285. New York: Springer-Verlag
19. M. Massoudi: Stability analysis of fluidized beds. Int. J. Engng Sci., **26** (1986)
20. I. Müller: On the entropy inequality. Arch. Rat. Mech. and Anal., **26** (1967), 118–141
21. I. Müller Thermodynamics, 1985, Pitman Advanced Publishing Program, Boston-London-Melbourne
22. J. W. Nunziato, S. L. Passman, & J. P. Thomas: Gravitational flow of granular materials with incompressible grains. J. Rheol., **24** (1980), 395–420
23. S. L. Passman, J. W. Nunziato, & E. K. Walsh (1984) A theory of multiphase mixtures. In: C. Truesdell (ed): Rational thermodynamics, pp 286–325. New York: Springer-Verlag
24. S. L. Passman, J. W. Nunziato, & P. B. Bailey: Shearing motion of a fluid-saturated granular material. J. Rheol., **30** (1986), 167–192
25. S. B. Savage: Gravity flow of cohesionless granular materials in chutes and channels. J. Fluid Mech., **92**(1) (1979), 53–96
26. B. Svendsen & K. Hutter: On the thermodymics of a mixture of isotropic materials with constraints. Int. J. Engng Sci., **33** (1995), 2021–205
27. B. Svendsen: A thermodynamic model for volume-fraction-based mixtures Z. Angew. Math. Mech., **77** (1997)
28. T. Takahashi: Debris flow. Ann. Rev. Fluid Mech., **13** (1991), 57–77
29. C. Truesdell: A new definition of a fluid, II: The Maxwellian fluid. Journal de Mathématiques Pures et Appliquées (9), **30** (1951), 111–155
30. C. Truesdell: Rational thermodynamics, 1969 New York, McGraw-Hill
31. Y. Wang & K. Hutter: Shearing flows in a Goodman-Cowin type granular material – Theory and numerical results. J. Particulate Technology (1998). in press
32. K. Wilmanski: The thermodynamical model of compressible porous materials with the balance equation of porosity. Preprint No. 310 (1997), Edited by Weierstraß-Institute für Angewandte Analysis und Stochastik, Berlin